ORIGINAL ARTICLE

Chloroplasts play a central role in facilitating MAMP-triggered immunity, pathogen suppression of immunity and crosstalk with abiotic stress

Susan Breen[1] | Rana Hussain[1] | Emily Breeze[1] | Hannah Brown[2] | Ibrahim Alzwiy[2] | Sara Abdelsayed[1,3] | Trupti Gaikwad[1] | Murray Grant[1]

[1]School of Life Sciences, University of Warwick, Coventry, UK

[2]School of Biosciences, College of Life and Environmental Sciences, University of Exeter, Exeter, UK

[3]Botany Department, Faculty of science, Benha University, Benha, Egypt

Correspondence
Murray Grant, School of Life Sciences, University of Warwick, Coventry CV4 7AL, UK.
Email: m.grant@warwick.ac.uk

Present address
Hannah Brown, Department of Health and Social Care, Victoria Street, London SW1H 0EU, UK.

Ibrahim Alzwiy, Authority of Natural Science Research and Technology, P.O. Box 30666, Tripoli, Libya.

Trupti Gaikwad, Marine Biology Association, Plymouth PL1 2PB, UK.

Funding information
Biotechnology and Biological Sciences Research Council

Abstract

Microbe-associated molecular pattern (MAMP)-triggered immunity (MTI) research has traditionally centred around signal transduction pathways originating from activated membrane-localized pattern recognition receptors (PRRs), culminating in nuclear transcription and posttranslational modifications. More recently, chloroplasts have emerged as key immune signalling hubs, playing a central role in integrating environmental signals. Notably, MAMP recognition induces chloroplastic reactive oxygen species (cROS) that is suppressed by pathogen effectors, which also modify the balance of chloroplast-synthesized precursors of the defence hormones, jasmonic acid, salicylic acid (SA) and abscisic acid. This study focuses on how well-characterized PRRs and coreceptors modulate chloroplast physiology, examining whether diverse signalling pathways converge to similarly modulate chloroplast function. Pretreatment of receptor mutant plants with MAMP and D(Damage)AMP peptides usually protect against effector modulation of chlorophyll fluorescence and prevent *Pseudomonas syringae* effector-mediated quenching of cROS and suppression of maximum dark-adapted quantum efficiency (the ratio of variable/maximum fluorescence [F_v/F_m]). The MTI coreceptor double mutant, *bak1-5/bkk1-1*, exhibits a remarkable decrease in F_v/F_m compared to control plants during infection, underlining the importance of MTI-mediated signalling in chloroplast immunity. Further probing the role of the chloroplast in immunity, we unexpectedly found that even moderate changes in light intensity can uncouple plant immune signalling.

KEYWORDS
chlorophyll fluorescence, chloroplast reactive oxygen, pattern recognition receptors, plant immunity

---

1 | INTRODUCTION

The plant immune system is multilayered and complex. It traditionally comprises three modules: microbe-associated molecular pattern (MAMP)-triggered immunity (MTI), effector-triggered immunity (ETI) and systemic acquired resistance (Jones & Dangl, 2006; Shine et al., 2019). The initial layer of defence, MTI, provides broad-spectrum defence against a diverse range of pathogens and has recently been shown to be involved in potentiating ETI responses, which can in turn reinforce MTI (Lu & Tsuda, 2021; Ngou et al., 2021; Nguyen et al., 2021; Yuan et al., 2021). Classical pathogen cell surface receptors comprise transmembrane receptor-like kinases (RLKs) or receptor-like proteins, including FLAGELLIN SENSING 2 (FLS2), EF-Tu RECEPTOR (EFR) and CHITIN ELICITOR RECEPTOR KINASE 1 (CERK1-2), which detect flagellin and elongation factor thermo-unstable (EF-Tu) from bacterial pathogens and chitin from fungi, respectively (Yu et al., 2017). However, an increasing number of MAMPs associated with a diverse range of pathogens have been identified (Noman et al., 2019). In addition, cell surface receptors can detect plant-derived damage-associated molecular patterns (DAMPs) found within extracellular spaces. Among DAMP receptors are the well-characterized RLKs, PEP RECEPTOR 1 (PEPR1) and PEPR2, which detect plant elicitor peptides, Peps. PEPR1 recognizes Peps1–6, while PEPR2 recognizes only Pep1 and Pep2 (Yamaguchi et al., 2006, 2010). These Peps are cleaved from the C-terminus of plant PROPEPs during cell damage and the transcripts of PROPEP1-3 are induced by defence-related hormones methyl salicylate and methyl jasmonate (Huffaker et al., 2006; Yamaguchi et al., 2010).

The pattern recognition receptors (PRRs), FLS2, EFR and PEPR1/2, are cell membrane-localized and contain extracellular leucine-rich repeat (LRR) surfaces where their ligands bind. Upon peptide detection by PRRs, coreceptors are recruited and bind to PRRs (and in some cases the ligand). The well-characterized coreceptor brassinosteroid-insensitive 1 (BRI1)-associated receptor kinase 1 (BAK1) belongs to the somatic embryogenesis RLK family (SERK), which contains five members, one of which, SERK4/BKK1 (BAK1-LIKE 1), has high sequence similarity to BAK1 and has functional redundancy (He et al., 2007). While BAK1 was first identified as a coreceptor for the BR receptor BRI1, involved in cell growth and division, it has become widely known for its role in plant immunity as plants containing the reduced function *bak1-5* allele have impaired FLS2, EFR and PEPR receptor function (Roux et al., 2011; Schwessinger et al., 2011). In contrast, *bkk1-1* still exhibits a reactive oxygen species (ROS) burst and mitogen-activated protein kinase (MAPK) (MPK3, MPK4 and MPK6) activation, which is comparable to wild-type plants, when treated with flg22 or elf18. However, the *bak1-5/bkk1-1* plants show minimal ROS and no MAPK activation in response to these MAMPs (Roux et al., 2011; Zipfel et al., 2006).

MTI triggers rapid calcium signalling, ROS and MAPK signalling cascades, all of which involve plasma membrane to nuclear signalling (Noman et al., 2019). Microbes successful in colonization secrete effectors to inter- or intracellular locations, which can dampen MTI signalling. Examples of such effector-triggered suppression (ETS) include the AvrPto effector from *Pseudomonas syringae*, which interacts with the PRRs FLS2 and EFR to dampen MTI in *Arabidopsis thaliana* (Xiang et al., 2008) and AvrE from *P. syringae* and the maize pathogen *Pantoea stewartii* subsp. *Stewartia*, which targets protein phosphatase 2 (PP2A) complexes to dampen MTI (Jin et al., 2016).

Effectors collectively target an array of plant immune signalling components, many of which still remain elusive. Some effectors are directly or indirectly recognized by cytoplasmic receptors, most often belonging to the nucleotide-binding leucine-rich repeat receptors (NLRs) class, activating a second immune response, ETI (Jones & Dangl, 2006). There are three major classes of NLRs, the first two classically defined by their N-terminal: Toll-like, interleukin-1 receptor domain TIR-NLRs (TNLs) and coiled-coil domain CC-NLRs (CNLs). More recently, the resistance to powdery mildew 8 CC-NLR class (Jones et al., 2016; Zhong & Cheng, 2016) have been described, which act as 'helper' NLRs for TNL and CNL 'sensor' NLRs (Lu & Tsuda, 2021; Maruta et al., 2022; Nguyen et al., 2021). Interaction of an effector and NLR is usually associated with the macroscopic development of the hypersensitive response, which restricts pathogen growth.

Classically, MTI research has centred around signal transduction pathways originating from the plasma membrane and activating nuclear transcription; however, it is becoming increasingly recognized that chloroplasts are a key hub of immune signalling (Kachroo et al., 2021; Littlejohn et al., 2021). Chloroplasts play a central role in integrating environmental signals and maintaining cellular homeostasis via retrograde signalling (Breeze & Mullineaux, 2022; de Souza et al., 2017). Relevant to host immune signalling, chloroplasts are also the site of chloroplastic ROS (cROS) generation and synthesis of defence hormone precursors, jasmonic acid (JA), salicylic acid (SA) and abscisic acid (ABA) (Littlejohn et al., 2021). A key early MTI response is the rapid ROS generation, an apoplastic localized respiratory burst, primarily generated by RBOHD, a member of the NADPH oxidase homolog (RBOH) family (Miller et al., 2009). Activating MTI using an effector secretion deficient strain of *P. syringae* pv. *tomato* strain DC3000 (DC3000*hrpA*) also rapidly generates cROS production in *A. thaliana*, which is attenuated in the virulent DC3000 strain, shortly after effector delivery (de Torres Zabala et al., 2015).

Concomitant with differences in cROS production during infection between the *P. syringae* strains DC3000 and DC3000*hrpA*, global transcriptome profiling of *A. thaliana* revealed significant alterations of nuclear-encoded chloroplast genes (*NECG*s). Remarkably, *NECG*s represent ~10% of all differentially up-regulated genes and ~30% of those significantly down-regulated (de Torres Zabala et al., 2015) during early MTI responses despite *NECG*s collectively accounting for only ~14% of the transcriptome. Superimposed on this, effector delivery (2–3 h postinfection; hpi) caused transcriptional reprogramming of *NECG*s, suggesting ETS also targets *NECG* expression (de Torres Zabala et al., 2015). These molecular signatures are reflected by physiological changes between DC3000 and DC3000*hrpA* challenge as evidenced by quantifying net photosynthetic CO_2 assimilation (A_{sat}) and chlorophyll fluorescence imaging

parameters associated with electron transport during photosynthesis. DC3000 but not DC3000*hrpA* challenge induced a decrease in CO_2 assimilation, maximum dark-adapted quantum efficiency (the ratio of variable/maximum fluorescence [F_v/F_m]), maximum operating efficiency of photosystem II (PSII) (F_v'/F_m') and the efficiency with which light absorbed by PSII is used for quinone acceptor (QA) reduction and linear electron transport (F_q'/F_m') (de Torres Zabala et al., 2015). In addition, DC3000 infection elicited an increase in nonphotochemical quenching (NPQ) and PSII redox state (qL; ($F_q'/F_v')/(F_o'/F')$)) compared to DC3000*hrpA* (de Torres Zabala et al., 2015). qL estimates the percentage of open PSII centres and the oxidation state of the primary PSII QA (Baker, 2008). An increase in qL suggests a decrease in electron transport from PSII. Thus, virulent pathogens can radically alter chloroplast physiological functions as part of their virulence strategy.

De novo induction of the plant hormone ABA during DC3000 infection contributes to ETS (de Torres Zabala et al., 2007) and was also recently shown to play a significant role in modulating chloroplast function. DC3000-induced suppression of F_v/F_m was accelerated by coinfiltration of 10 μM ABA, effectively phenocopying DC3000 challenge of the *Arabidopsis* ABA hypersensitive protein phosphatase 2C (PP2C) *abi1/abi2/hab1* triple mutant. By contrast, the ABA-deficient *Arabidopsis aldehyde oxidase 3* (*aao3*) mutant restricted DC3000 suppression of F_v/F_m (de Torres Zabala et al., 2015). Collectively, these data show that the chloroplast is targeted early in pathogen infection and before bacterial multiplication, with one of the earliest initial events being suppression of cROS.

This study focussed on how well-characterized MTI PRRs and coreceptors impacted chloroplast physiology, including accessing whether diverse signalling pathways converged to similarly modulate chloroplast function, using F_v/F_m as the primary readout. Here, we comprehensively examine chlorophyll fluorescence dynamics and the impact on attenuating chloroplast cROS. We show that pretreatment of receptor mutant plants with MAMP and DAMP peptides generally offer protection against effector modulation of chlorophyll fluorescence, but surprisingly, *fls2* plants pretreated with chitin fail to provide such protection. The double mutant of the MTI coreceptors *bak1-5/bkk1-1* exhibits a remarkable decrease in F_v/F_m compared to control plants during infection, highlighting the importance of MTI-mediated signalling in underpinning chloroplast immunity. Expanding these findings to better understand the role of ABA and abiotic stress in chloroplast immunity, we unexpectedly found that moderate light, representative of that found in the plant's natural environment outside the laboratory, overrides the protection offered by MAMPs on wild-type plants.

2 | MATERIALS AND METHODS

2.1 | *Arabidopsis* growth conditions

Arabidopsis thaliana seeds were sown in a compost mix comprising Levingston F2 compost + sand (LEV206):vermiculite (medium grade) mixed in a 6:1 ratio. Plants were grown in a controlled environment growth chamber under 10-h day (21°C; 120 μmol m⁻² s⁻¹) and 14-h night (21°C) with a relative humidity of 65% for 5–6 weeks before use.

2.2 | *Arabidopsis* peptide treatment

Pretreatment of plants was conducted 16 h before bacterial challenge, by infiltration of the peptide. Coinfiltration experiments were conducted by mixing the peptide or hormone of interest with the bacterial culture to attain the required final concentration and OD_{600} before infiltration. Concentrations of peptides or hormones were as follows: 1 μM of flg22, elf18, Pep1, Pep2 and Pep3; 100 μg ml⁻¹ of chitin (Sigma; C9752) and 10 or 100 μM ABA. H_2O was used as a mock for pretreatment.

2.3 | Bacterial growth, maintenance and inoculation

Pseudomonas syringae strains were grown on solid Kings B media containing appropriate antibiotics as described (King et al., 1954; Truman et al., 2006). For inoculation, overnight cultures were grown with shaking (200 rpm) at 28°C. Cells were harvested (1500*g* × 7 min), washed and resuspended in 10 mM $MgCl_2$. Cell density was adjusted to OD_{600} 0.15 (~0.75 × 10⁸ colony-forming units ml⁻¹) for fluorescence imaging and confocal microscopy or OD_{600} 0.0002 for growth assays. Bacteria were infiltrated into the leaves on the abaxial side using one infiltration site on each side of the midvein. All growth assays and ROS imaging experiments were performed at least three times. All fluorescence imaging experiments were performed at least four times.

2.4 | Chlorophyll fluorescence imaging

PSII chlorophyll fluorescence imaging of *Arabidopsis* rosettes was performed with a CF Imager (Technologica Ltd.). *Normal light cycle*: Plants were placed in the chamber for 40 min postinoculation and then dark adapted for 20 min. This was followed by a saturating light pulse (6349 μmol m⁻² s⁻¹ for 0.8 s) to obtain maximum dark-adapted fluorescence (F_m). Actinic light (120 μmol m⁻² s⁻¹—the same as plant growth light intensity) was then applied for 15 min, followed by a saturating pulse to obtain maximum light adapted fluorescence (F_m'). The plants remained in actinic light for a further 24 min and then returned to a dark period of 20 min. This cycle (59 min duration) was repeated 23 times. *Moderate light cycle*: plants were placed in the chamber for 40 min postinoculation and then dark adapted for 20 min. This was followed by a saturating light pulse (6349 μmol m⁻² s⁻¹ for 0.8 s) to obtain maximum dark-adapted fluorescence (F_m). Moderate light (650 μmol m⁻² s⁻¹) was then applied for 15 min, followed by three saturating light pulses 5 min

apart to obtain maximum light-adapted fluorescence (F_m'). The plants remained in moderate light for a further 150 min and then were returned to a 20 min dark phase. This cycle (200 min duration) was repeated eight times. F_m, F_m' and F_o (minimal fluorescence with fully oxidized PSII centres) were used to calculate chlorophyll fluorescence parameters related to PSII: F_v/F_m (maximum dark-adapted quantum efficiency) and NPQ. These values were calculated as described by (Baker, 2008).

2.5 | Bacterial growth measurements

Three leaves per plant (six plants total) were syringe infiltrated on the abaxial side using one infiltration site on each side of the midvein with bacteria, OD_{600} 0.0002 and placed either under moderate light (450 or 600 μmol m^{-2} s^{-1}) or normal light (120 μmol m^{-2} s^{-1}) for 4 days. Three independent leaf discs per plant were excised and homogenized using a Tissue Lyser (Qiagen). Serial dilutions were spotted on Kings B media and colonies were counted at 24 hpi.

2.6 | Confocal microscopy

Col-0 plants were pretreated with either water or peptide 16 h before bacterial challenge and then 3.5 hpi leaves were detached and floated, adaxial surface upwards, in a solution of 10 mM MgCl$_2$ containing 10 μM (Enzo) for 40min and then washed for 20 min in 10 mM MgCl$_2$ before imaging. Samples were mounted in perfluorodecalin (Littlejohn et al., 2010) and images were captured on a Zeiss 880 using a ×40 oil immersion lens. Argon laser excitation at 488 nm and an emission window of 512–527 nm was used to capture the dichlorofluorescein (DCF) signal. Chloroplast fluorescence was measured at 659–679 nm.

3 | RESULTS

3.1 | MAMP pretreatment protects F_v/F_m suppression by *P. syringae* DC3000 infection

Previous work showed that leaves pretreated with flg22 24 hpi with virulent *P. syringae* DC3000-restricted effector-induced suppression of maximum dark-adapted quantum efficiency (F_v/F_m) levels (de Torres Zabala et al., 2015). To determine if this observation was true for other peptide elicitors, wild-type, Col-0, *A. thaliana* leaves were pretreated with the bacterial peptides flg22 (1 μM), elf18 (1 μM) and the fungal peptide chitin (chi; 100 μg ml^{-1}) and then challenged with DC3000 at 16 hpi. All pretreatment-protected challenged leaves from DC3000-induced suppression of F_v/F_m over a 24-h period (Figure 1a). Figure 1b illustrates F_v/F_m images at 18 hpi showing pretreated leaves (flg, elf, chi) have healthy F_v/F_m responses (red/orange false-coloured leaves), whereas reduced F_v/F_m due to

DC3000 infection following H$_2$O (mock) pretreatment is indicated by their distinctive green/blue false colouration.

Flg22, elf18 and chitin are recognized by the plant cell surface PRRs FLS2, EFR and Cerk1-2, respectively. Elf18 pretreatment of *fls2* leaves primed the plant and this crossprotection resulted in no change to F_v/F_m during DC3000 infection (de Torres Zabala et al., 2015). These data indicate that activation of different MTI receptors can abrogate effector-mediated F_v/F_m suppression. Consistent with this hypothesis, flg22 pretreatment on *efr1* (Figure 1c,d) or *cerk1-2* leaves (Figure 1e,f) results in a protection against DC3000 mediated F_v/F_m suppression over a 24 h period. The level of protection offered by flg22 to *efr1* and *cerk1-2* mutants is comparable to the Col-0 control (Figure 1c,e). By contrast, pretreatment of elf18 on *efr1* plants (Figure 1c,d) and chitin on *cerk1-2* plants (Figure 1e,f) failed to prevent suppression of F_v/F_m following DC3000 infection. The F_v/F_m images at 18 hpi illustrate healthy (red/orange) flg22-pretreated leaves on Col-0, *efr1* and *cerk1-2* plants compared to suppression of F_v/F_m (green/blue) induced by DC3000 infection (Figure 1d,f) following H$_2$O treatment. In addition, elf18 pretreatment protects *cerk1-2* plants from reduced F_v/F_m during DC3000 infection (Figure 2a,b). Notably, *cerk1-2*-challenged leaves showed greater suppression of F_v/F_m compared to Col-0 (Figures 1d and 2a), indicating uncoupling chitin signalling may also weaken chloroplast immune responses. Surprisingly, while pretreatment of *efr1* plants with chitin protected them from DC3000-induced suppression of F_v/F_m levels, chitin pretreatment failed to protect *fls2* plants during DC3000 infection (Figure 2c,d), where DC3000 suppression of F_v/F_m was indistinguishable from H$_2$O pretreatment (Figure 2e,f).

3.2 | MAMP pretreatment compromises effector-induced suppression of cROS

cROS are products of photosynthetic electron transport, comprising singlet oxygen ($^1O_2$), hydrogen peroxide (H_2O_2) and superoxide anions ($O_2^{\bullet-}$), with $O_2^{\bullet-}$ and $^1O_2$ being produced under high light stress at PSI and PSII respectively (Foyer & Hanke, 2022). The MTI-induced cROS burst has emerged as an important component of plant immunity, as evidenced by early DC3000 effector delivery to attenuate this process (de Torres Zabala et al., 2015). Therefore, we first assessed the relationship between F_v/F_m and cROS production and the role of DC3000 effectors in these processes by treating leaves with the nonspecific ROS reporter, 2′,7′-dichlorodihydrofluorescein diacetate (H$_2$DCF-DA) and imaging cROS following DC3000 infection. Strong cROS induction following DC3000*hrpA* infection (MTI) was evident at 4.5 hpi, whereas cROS was minimal in DC3000-challenged (ETS) leaves at this time (Figure 3a,b). Notably, flg22 or elf18 pretreatment of leaves before DC3000 challenge generated cROS at 4.5 hpi (Figure 3c,d), indicating that the effectors secreted during DC3000 infection could not dampen cROS within a primed leaf.
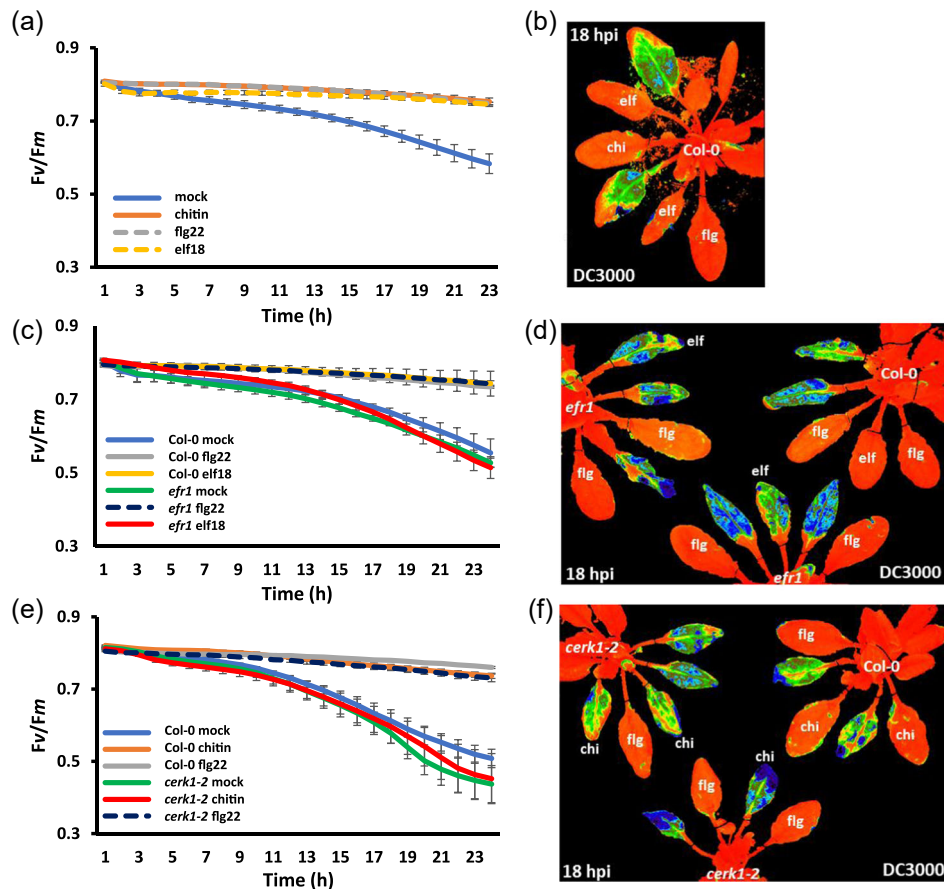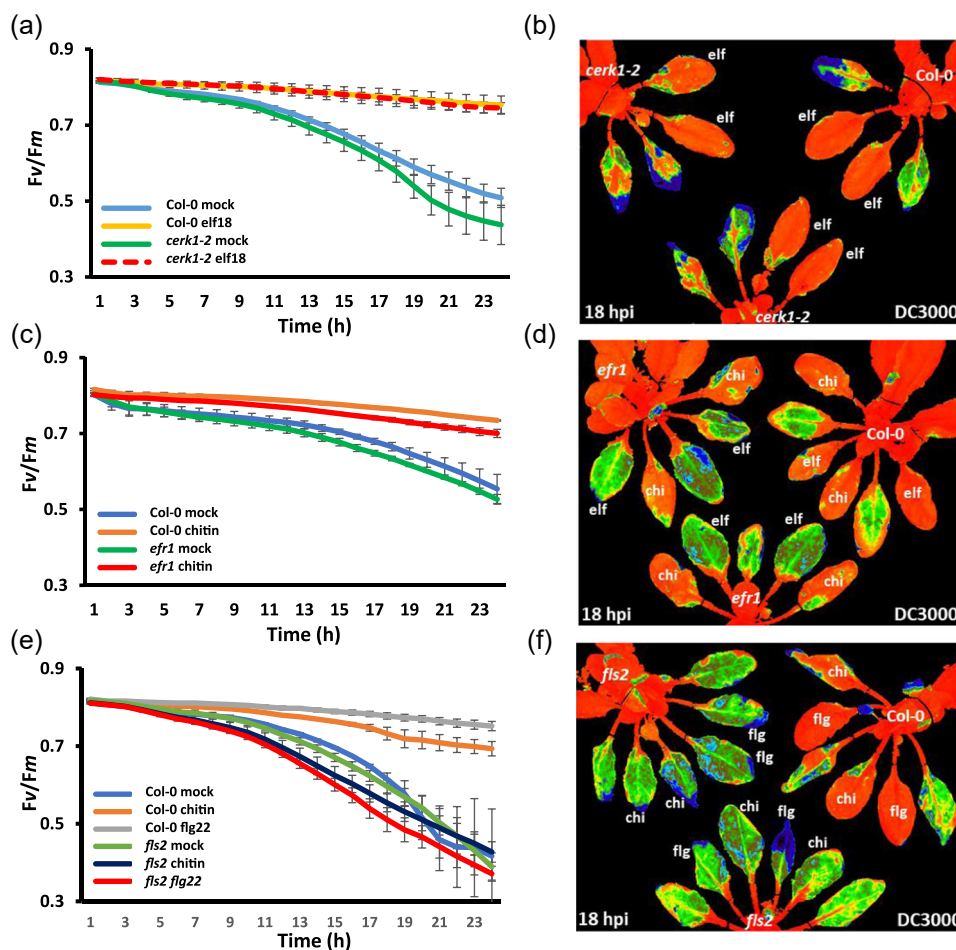
FIGURE 1 Microbe-associated molecular pattern (MAMP) pretreatment protects the ratio of variable/maximum fluorescence (F_v/F_m) from bacterially induced suppression. MAMP pretreatment was infiltrated 16 h before bacterial challenge with bacteria infiltrated into the leaves on the abaxial side using one infiltration site on either side of the leaf midvein. (a) Graph quantifying changes in F_v/F_m over 23 hours postinfection (hpi) with DC3000 infection on Col-0 leaves. Blue line represents leaves pretreated with H_2O; orange—pretreated with chitin (100 µg ml^{-1}); dashed grey—leaves pretreated with flg22 (1 µM) and dashed yellow—leaves pretreated with elf18 (1 µM). (b) The 18 hpi false-coloured image F_v/F_m of a Col-0 plant pretreated with H_2O, chitin (100 µg/ml), flg22 (1 µM) and elf18 (1µM) at 18 hpi with DC3000. Orange represents normal F_v/F_m, whereas yellow/green/blue represents suppressed F_v/F_m. (c) Graph quantifying changes in F_v/F_m over 24 h following DC3000 infection on Col-0 and *efr1* leaves. Blue line represents Col-0 leaves pretreated with H_2O; grey—Col-0 leaves pretreated with flg22 (1 µM); yellow—Col-0 leaves pretreated with elf18 (1 µM); green—*efr1* leaves pretreated with H_2O; dashed blue—*efr1* leaves pretreated with flg22 (1 µM); red—*efr1* leaves pretreated with elf18 (1 µM). (d) False-coloured visual snapshot of F_v/F_m for a Col-0 plant (top right) and *efr1* plants pretreated with H_2O, flg22 (1 µM) and elf18 (1 µM) at 18 hpi with DC3000. Orange represents normal F_v/F_m, whereas yellow/green/blue represents suppressed F_v/F_m. (e) Graph quantifying changes in F_v/F_m over 24 h of DC3000 infection on Col-0 and *cerk1-2* leaves. Blue represent Col-0 leaves pretreated with H_2O; orange—Col-0 leaves pretreated with chitin (100 µg ml^{-1}); grey—Col-0 leaves pretreated with flg22 (1 µM); green—*cerk1-2* leaves pretreated with H_2O; red—*cerk1-2* leaves pretreated with chitin (100 µg ml^{-1}) and dashed blue—*cerk1-2* leaves pretreated with flg22 (1 µM). (f) The 18 hpi false-coloured image of F_v/F_m for Col-0 (top right) and *cerk1-2* plants pretreated with H_2O, flg22 (1 µM) and chitin (100 µg ml^{-1}) challenged with DC3000. Orange represents normal F_v/F_m, whereas yellow/green/blue represents suppressed F_v/F_m. Flg22; flg: chitin; chi: elf18; elf.

3.3 | *bkk1-1/bak1-5* plants show hyper suppression of F_v/F_m during *P. syringae* DC3000 infection

As primary PRRs mediate chloroplast immune signals, the cell surface coreceptor mutants *bak1-5*, *bkk1-1* and double mutant *bkk1-1/bak1-5* were used to assess their contribution to altered F_v/F_m dynamics during DC3000 infection. *bkk1-1* plants pretreated with flg22, elf18 and chitin 16 h before infection with DC3000

showed F_v/F_m infection signatures equivalent to those measured following DC3000*hrpA* infection in Col-0 plants (Figure 4a–c and Supporting Information: Figure 1a,b). DC3000-challenged *bak1-5* plants showed a small but significantly greater suppression of F_v/F_m compared to Col-0 (Figure 4d), as expected given its partial loss of MTI function (Roux et al., 2011). These data highlight both the power of quantitative chlorophyll fluorescence measurements and the ability to dynamically monitor effector impact on chloroplast physiology. Interestingly, F_v/F_m dynamics in DC3000*hrpA*
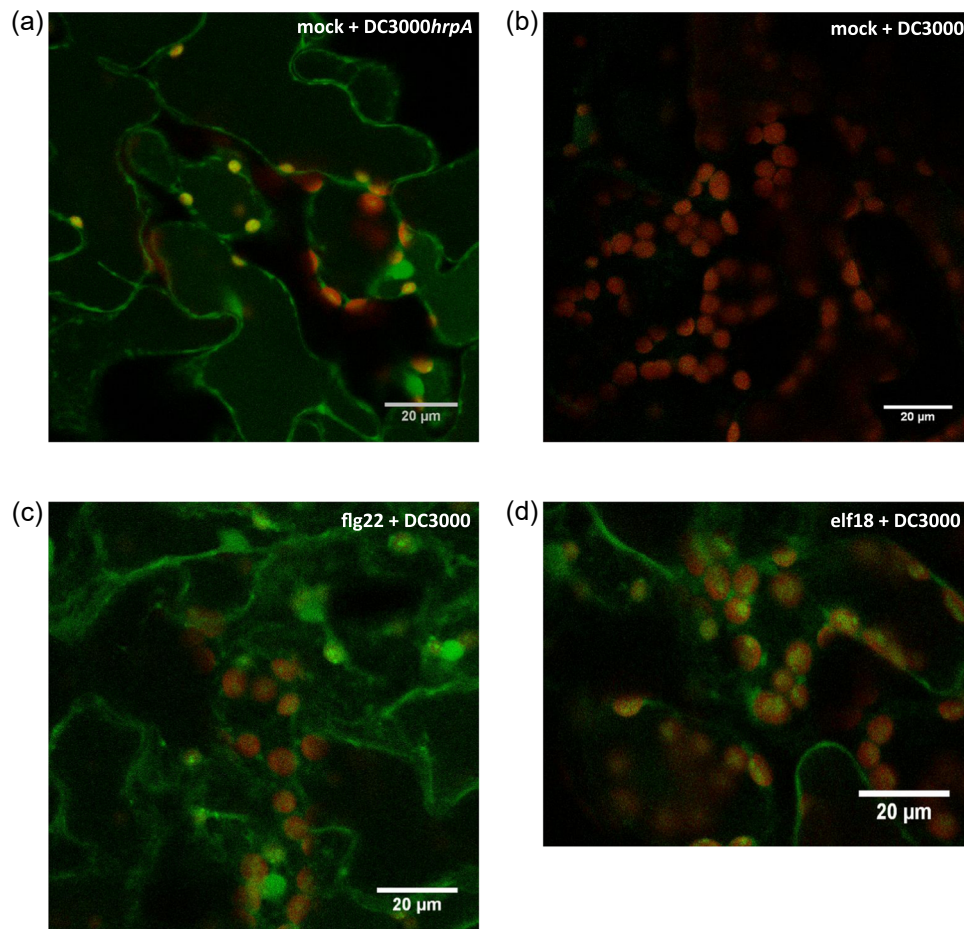
FIGURE 2 Microbe-associated molecular pattern (MAMP) pretreatment protects the ratio of variable/maximum fluorescence (F_v/F_m) from bacterially induced suppression, with the exception of chitin pretreatment of *fls2* leaves. MAMP pretreatment was infiltrated 16 h before bacterial challenge, bacteria were infiltrated into the leaves on the abaxial side using one infiltration site on either side of the leaf midvein. (a) Graph quantifying changes in F_v/F_m over 24 hours postinfection (hpi) with DC3000 on Col-0 and *cerk1-2* leaves. Blue line represents Col-0 leaves pretreated with H_2O; yellow—Col-0 leaves pretreated with elf18 (1 µM); green—*cerk1-2* leaves pretreated with H_2O and dashed red line—*cerk1-2* leaves pretreated with elf18 (1 µM). (b) Representative visual false-coloured snapshot of F_v/F_m for a Col-0 plant (top right) and *cerk1-2* plants pretreated with H_2O and elf18 (1 µM) at 18 hpi with DC3000. Orange represents normal F_v/F_m, whereas yellow/green/blue represents suppressed F_v/F_m. (c) Graph quantifying changes in F_v/F_m over 24 h of DC3000 infection on Col-0 and *efr1* leaves. Blue represents Col-0 leaves pretreated with H_2O; orange—Col-0 leaves pretreated with chitin (100 µg ml^{-1}); green—*efr1* leaves pretreated with H_2O and red—*efr1* leaves pretreated with chitin (100 µg ml^{-1}). (d) Visual false-coloured snapshot of F_v/F_m for a Col-0 plant (top right) and *efr1* plants pretreated with H_2O and chitin (100 µg ml^{-1}) at 18 hpi with DC3000. Orange represents normal F_v/F_m, whereas yellow/green/blue represents suppressed F_v/F_m. (e) Graph quantifying changes in F_v/F_m over 24 h of DC3000 infection on Col-0 and *fls2* leaves. Blue represent Col-0 leaves pretreated with H_2O; orange—Col-0 leaves pretreated with chitin (100 µg ml^{-1}); grey—Col-0 leaves pretreated with flg22 (1 µM); green—*fls2* leaves pretreated with H_2O; dark blue—*fls2* leaves pretreated with chitin (100 µg ml^{-1}) and red—*fls2* leaves pretreated with flg22 (1 µM). (f) False-coloured image of F_v/F_m for a Col-0 plant (top right) and *fls2* plants pretreated with H_2O, chitin (100 µg ml^{-1}) and flg22 (1 µM) at 18 hpi with DC3000. Orange represents normal F_v/F_m, whereas yellow/green/blue represents suppressed F_v/F_m. [Color figure can be viewed at wileyonlinelibrary.com]

challenged *bak1-5* leaves pretreated with flg22 or elf18 before infection were wild type in response, whereas chitin pretreatment only partially protected against F_v/F_m suppression in the *bak1-5* background (Figure 4d–f and Supporting Information: Figure 1c,d). Strikingly, MAMP pretreatment with flg22, elf18 or chitin had no protective effect on F_v/F_m dynamics in the *bkk1-1/bak1-5* double mutant with F_v/F_m suppression being identical and often greater than the respective Col-0 control treatment (Figure 4e–g and Supporting Information: Figure 1d,e).

3.4 | Pretreatment of leaves with DAMPs results in the protection of F_v/F_m during *P. syringae* DC3000 infection

Given the protection offered by MAMPs to F_v/F_m levels during DC3000 infection, we next tested whether similar protection was also conferred by plant-derived DAMPs. Using Pep elicitors, Col-0 leaves were first pretreated with Pep1, Pep2 or Pep3 (all at 1 µM) 16 h before DC3000 challenge. F_v/F_m dynamics over 24 h revealed that Pep1 and 3 but not

FIGURE 3 DC3000 is unable to suppress chloroplastic reactive oxygen species in microbe-associated molecular pattern (MAMP) pretreatment leaves. MAMP pretreatment was infiltrated 16 h before bacterial challenge and bacteria were infiltrated into the leaves on the abaxial side using one infiltration site on either side of the leaf midvein. Col-0 leaves treated with the nonspecific species stain 2′,7′-dichlorodihydrofluorescein diacetate 5.5 hours postinfection (hpi) with DC3000hrpA and DC3000. Leaves were imaged on a Zeiss 880 confocal microscope using excitation at 488 nm and an emission window of 512–527nm to capture the oxidized dichlorofluorescein signal (green). Chloroplast fluorescence was measured at 659–679 nm (red). Scale bars = 20 μm. (a) H$_2$O pretreated and DC3000hrpA infection. (b) H$_2$O pretreated and DC3000 infection. (c) flg22 (1 μM) pretreated and DC3000 infection. (d) elf18 (1 μM) pretreated and DC3000 infection. Image representative of three biological replicates. [Color figure can be viewed at wileyonlinelibrary.com]

Pep2 protected from DC3000 F_v/F_m suppression (Figure 5a,b). Critically, Pep1 and 3 pretreatment failed to alter DC3000 F_v/F_m infection dynamics in the *pepR1-1 × 2-1* mutant (Yamaguchi et al., 2010) (Figure 5c,d), whereas flg22 pretreated *pepR1-1 × 2-1* leaves protected from F_v/F_m suppression as described above for Col-0 flg22 pretreatment (Figure 5e,f). Interestingly, Pep1 and Pep3 pretreatment only provided partial protection against F_v/F_m suppression in DC3000 infected *fls2* leaves and no protection in *bkk1-1/bak1-5* plants (Supporting Information: Figure 2a–d). These data indicate a degree of crossprotection of F_v/F_m between DAMPs and MAMP priming of the plant.

3.5 | Moderate light enhances F_v/F_m reduction during *P. syringae* DC3000 infection

Numerous studies have looked at plant acclimation to high light, typically 1000–3000 μmol m^{-2} s^{-1}. Excess light can be absorbed by the light-harvesting complexes and dissipated as heat via thermal energy dissipation, linked to NPQ mechanisms (Holt et al., 2004). Excess light also modulates both ROS and phytohormones. Crosstalk between ROS- and SA-dependent pathways has been shown to regulate both light acclimation and defence responses leading to pathogen resistance, as reviewed in Kangasjarvi et al. (2012, 2013).

Light levels typically used in *Arabidopsis*–pathogen interactions are significantly lower than those used for studying acclimation to excess excitation energy, tending to be of relatively low light intensity (80–150 mol m^{-2} s^{-1}). Outside the laboratory, light levels are usually substantially higher than those and often fluctuating, thus requiring a dynamic response from the photosynthetic apparatus via an array of homeostatic control mechanisms that modulate changes in cellular energy and reductant status (Kangasjarvi et al., 2012) and retrograde signalling (Szechyńska-Hebda & Karpiński, 2013).

To explore the impact of 'moderate' light levels (300–600 μmol m^{-2} s^{-1}), we examined F_v/F_m dynamics during DC3000
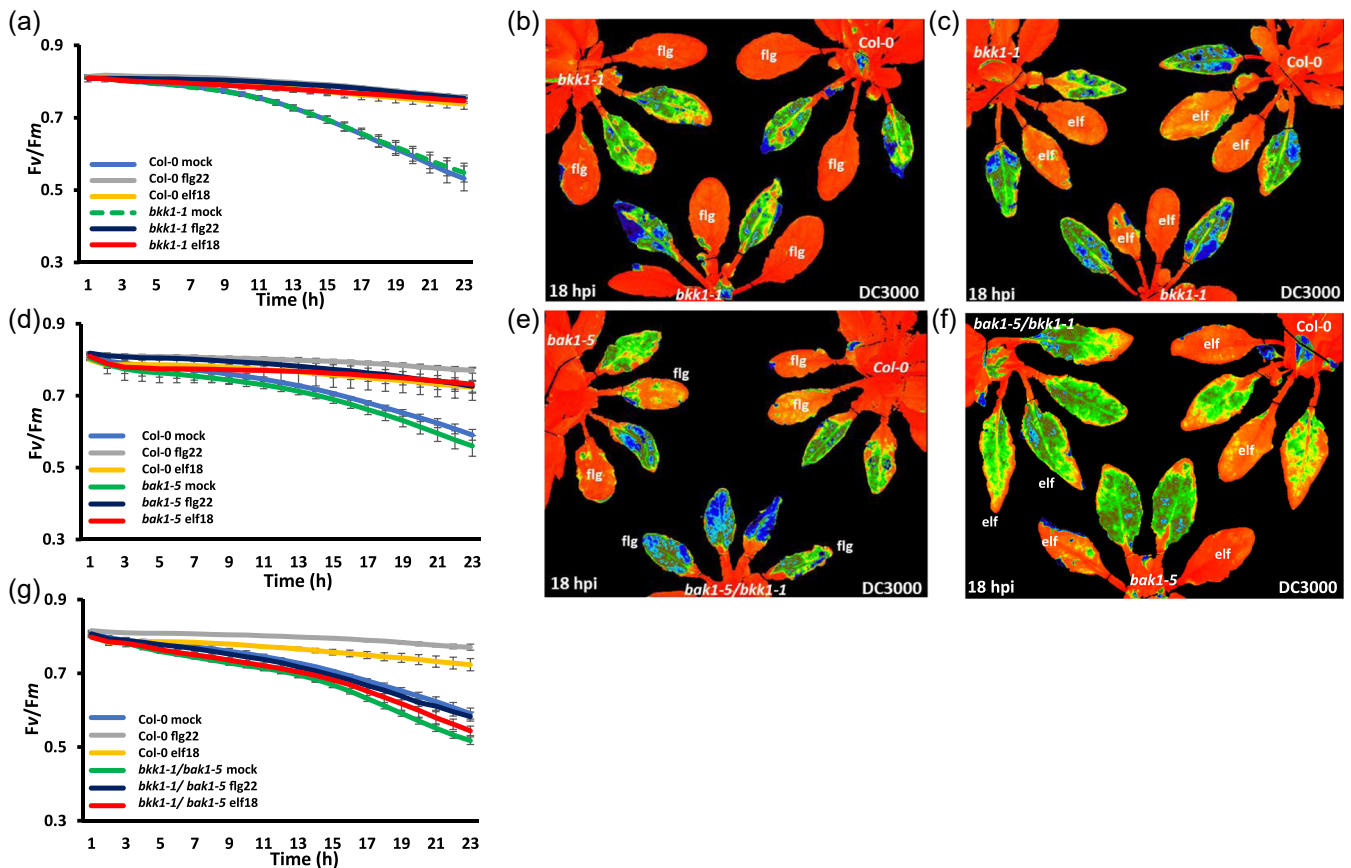
FIGURE 4 Bacterial microbe-associated molecular pattern (MAMP) pretreatments provide full and partial protection on *bkk1-1* and *bak1-5* single mutant lines but fail to protect *bak1-5/bkk1-1* lines. MAMP pretreatment was infiltrated 16 h before bacterial challenge and bacteria were infiltrated into the leaves on the abaxial side using one infiltration site on either side of the leaf midvein. (a) Graph quantifying changes in the ratio of variable/maximum fluorescence (F_v/F_m) over 23 h of DC3000 infection on Col-0 and *bkk1-1* leaves. Blue line represents Col-0 leaves pretreated with H_2O; grey—Col-0 leaves pretreated with flg22 (1 µM); yellow—Col-0 leaves pretreated with elf18 (1 µM); green dashed line—*bkk1-1* leaves pretreated with H_2O; dark blue—*bkk1-1* leaves pretreated with flg22 (1 µM); red—*bkk1-1* leaves pretreated with elf18 (1 µM). (b) False-coloured image, 18 hours postinfection (hpi) with DC3000, of F_v/F_m for Col-0 (top right) and *bkk1-1* plants pretreated with H_2O and flg22 (1 µM). (c) False-coloured image, 18 hpi with DC3000, of F_v/F_m for Col-0 (top right) and *bkk1-1* plants pretreated with H_2O and elf18 (1 µM). Orange represents normal F_v/F_m, whereas yellow/green/blue represents suppressed F_v/F_m. (d) Graph quantifying changes in F_v/F_m over 23 hpi with DC3000 on Col-0 and *bak1-5* leaves. Blue represents Col-0 leaves pretreated with H_2O; grey—Col-0 leaves pretreated with flg22 (1 µM); yellow—Col-0 leaves pretreated with elf18 (1 µM); green—*bak1-5* leaves pretreated with H_2O; dark blue—*bak1-5* leaves pretreated with flg22 (1 µM); red corresponds to *bak1-5* leaves pretreated with elf18 (1 µM). (e) False-coloured image at 18 hpi with DC3000, of F_v/F_m for Col-0 (top right), *bak1-5* (top left) or *bak1-5/bkk1-1* (bottom), plants pretreated with H_2O and flg22 (1 µM). (f) False-coloured image, 18 hpi with DC3000, of F_v/F_m for Col-0 (top right), *bak1-5* (bottom) or *bak1-5/bkk1-1* (top left), plants pretreated with H_2O and elf18 (1 µM) at 18 hpi with DC3000. Orange represents normal F_v/F_m, whereas yellow/green/blue represents suppressed F_v/F_m. (g) Quantitative changes in F_v/F_m over 23 hpi with DC3000 on Col-0 and *bak1-5/bkk1-1* leaves. Blue represents Col-0 leaves pretreated with H_2O; grey—Col-0 leaves pretreated with flg22 (1 µM); yellow—Col-0 leaves pretreated with elf18 (1 µM); green—*bak1-5/bkk1-1* leaves pretreated with H_2O; dark blue—*bak1-5/bkk1-1* leaves pretreated with flg22 (1 µM); red—*bak1-5/bkk1-1* leaves pretreated with elf18 (1 µM). [Color figure can be viewed at wileyonlinelibrary.com]

infection under standard growth conditions (normal light) or moderate light conditions. A 'normal' light (120 µmol m^{-2} s^{-1}) cycle of 1 h (as above) comprised 40 min of light before dark adaption for 24 cycles. To ensure the duration of moderate light exposure would encompass early pathogen infection events, including expression of effector genes and assembly of the Type-III secretion system (T3SS), we used a regime of 2.5 h moderate light (650 µmol m^{-2} s^{-1}) before dark adaption, enabling F_v/F_m measurements to be captured eight times over a 26 h period. In comparison to DC3000 or DC3000*hrpA*

challenge under normal light conditions (Figure 6a,b), moderate light resulted in a dramatic initial decrease of F_v/F_m within the first 6.5 hpi for both DC3000 and DC3000*hrpA* challenges. F_v/F_m in DC3000*hrpA*-treated leaves partially recovered and did not regain levels observed under normal light conditions (Figure 6c,d). By contrast, leaves infected with DC3000 showed strong decreases in F_v/F_m over the entire 26 h. These were consistently significantly lower than that observed in infected leaves under normal light (Figure 6a–d). Interestingly, at 650 µmol m^{-2} s^{-1}, flg22 and elf18
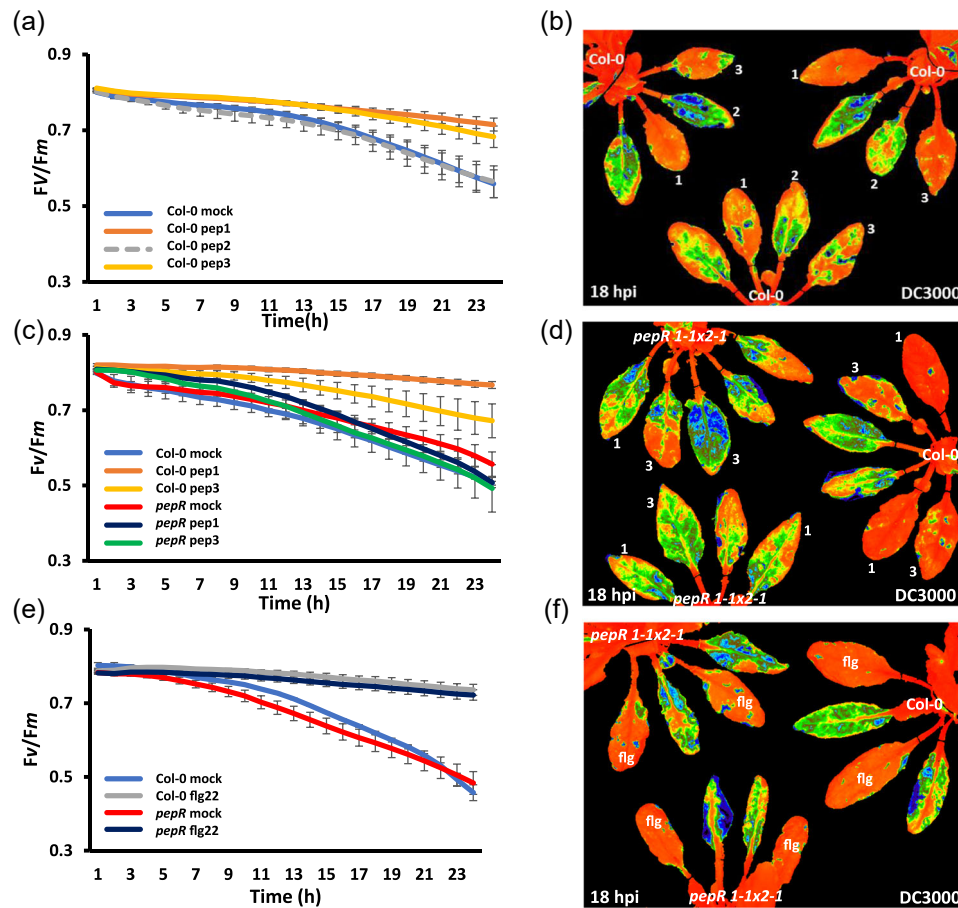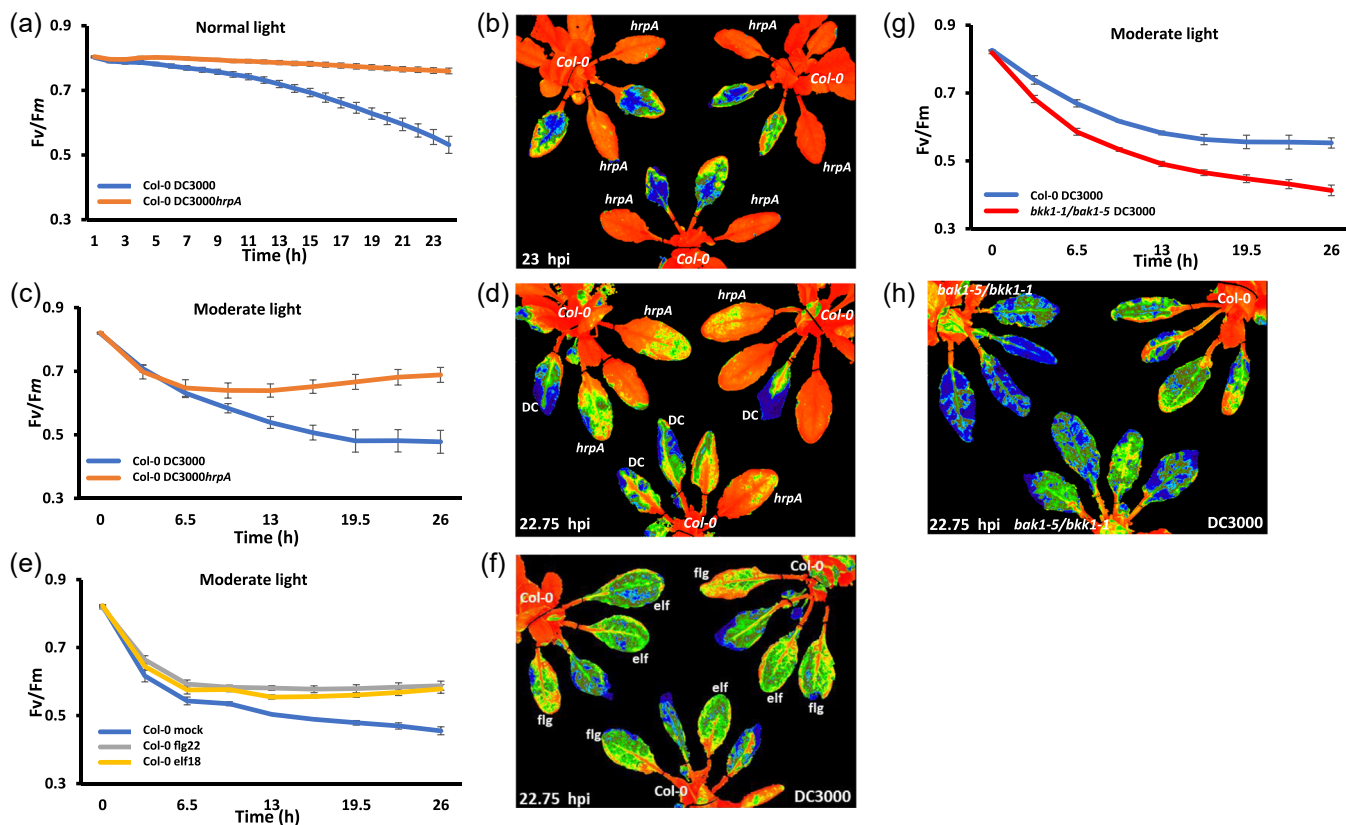
FIGURE 5 Damage-associated molecular pattern (DAMP) pretreatment restricts suppression of the ratio of variable/maximum fluorescence (F_v/F_m) following bacterial challenge. DAMP pretreatment was infiltrated 16 h before bacterial challenge and bacteria were infiltrated into the leaves on the abaxial side using one infiltration site either side of the leaf midvein. (a) Graph quantifying changes in F_v/F_m over 24 hours postinfection (hpi) following DC3000 infection of Col-0. Blue represents leaves pretreated with H_2O; orange—pretreated with Pep1 (1 µM); dashed grey—pretreated with Pep2 (1 µM); yellow—pretreated with Pep3 (1 µM). (b) False-coloured image of F_v/F_m in Col-0 plants pretreated with H_2O, Pep1 (1 µM), Pep2 (1 µM) or Pep3 (1 µM) at 18 hpi with DC3000. Orange represents normal F_v/F_m, whereas yellow/green/blue represents suppressed F_v/F_m. (c) Graph quantifying changes in F_v/F_m over 24 hpi with DC3000 on Col-0 and $pepR1-1 \times 1-2$ leaves. Blue represents Col-0 leaves pretreated with H_2O; orange—Col-0 pretreated with pep1 (1 µM); yellow—Col-0 pretreated with pep3 (1 µM); red—$pepR1-1 \times 1-2$ pretreated with H_2O; dark blue—$pepR1-1 \times 1-2$ pretreated with pep1 (1 µM); green—$pepR1-1 \times 1-2$ leaves pretreated with pep3 (1 µM). (b) False-coloured image of F_v/F_m for Col-0 (right) and $pepR1-1 \times 1-2$ pretreated with H_2O, Pep1 (1 µM) and Pep3 (1µM) 18 hpi with DC3000. Orange represents normal F_v/F_m, whereas yellow/green/blue represents suppressed F_v/F_m. (e) Graph quantifying changes in F_v/F_m over 24 hpi with DC3000 on Col-0 and $pepR1-1 \times 1-2$ leaves. Blue represents Col-0 leaves pretreated with H_2O; grey—Col-0 leaves pretreated with flg22 (1 µM); red—$pepR1-1 \times 1-2$ leaves pretreated with H_2O and dark blue—$pepR1-1 \times 1-2$ leaves pretreated with flg22 (1 µM). (f) Representative false-coloured image, 18 hpi with DC3000, of F_v/F_m for Col-0 (right) and $pepR1-1 \times 1-2$ plants pretreated with H_2O and flg22 (1 µM). Orange represents normal F_v/F_m, whereas yellow/green/blue represents suppressed F_v/F_m. [Color figure can be viewed at wileyonlinelibrary.com]

pretreatment failed to prevent the majority of the suppression of F_v/F_m and, in fact, showed infection dynamics very similar to that observed in DC3000 challenged Col-0 leaves. These data imply this moderately increased light alone was sufficient to drive enhanced F_v/F_m suppression by DC3000 (Figure 6e,f), and strikingly, further suppress the F_v/F_m infection dynamics observed in DC3000 challenged *bkk1-1/bak1-5* leaves (Figure 6g,h).

To ascertain the impact of moderate light on host susceptibility, we enumerated bacterial growth under 120 or 450 µmol m^{-2} s^{-1} light regimes. As the strong F_v/F_m suppression under moderate light

exhibited by the DC3000 challenge is reminiscent of ETI responses (Littlejohn et al., 2021), it was surprising that 450 µmol m^{-2} s^{-1} (<4-fold increase in intensity) enhanced susceptibility (Figure 7 and Supporting Information: Figure 3b). Interestingly, already hyper-susceptible *bkk1-1/bak1-5* plants were even more susceptible to DC3000 infection at 450 µmol m^{-2} s^{-1}, suggesting that this moderate light intensity uncouples immunity through pathways independently of those guarded by classical MTI signalling (Figure 7), and/or that MTI signalling is less effective at increased light intensity. There was, however, no significant difference in bacterial growth observed for

FIGURE 6 Moderate light enhances bacterial suppression of the ratio of variable/maximum fluorescence (F_v/F_m). Bacteria were infiltrated into the leaves on the abaxial side using one infiltration site on either side of the leaf midvein, where undertaken microbe-associated molecular pattern (MAMP) Pretreatment was infiltrated 16 h before bacterial challenge. (a) Graph quantifying changes in F_v/F_m over 24 hours postinfection (hpi) of DC3000 (blue line) and DC3000hrpA (orange line) infection on Col-0 leaves under normal light (NL) (120 µmol m^{-2} s^{-1}). (b) False-coloured image of F_v/F_m at 23 hpi of Col-0 plants with DC3000 and DC3000hrpA under NL (120 µmol m^{-2} s^{-1}). Orange represents the expected F_v/F_m, whereas yellow/green/blue represents suppressed F_v/F_m. (c) Graph quantifying changes in F_v/F_m over 26.5 hpi of DC3000 (blue line) and DC3000hrpA (orange line) infection on Col-0 leaves under moderate light (650 µmol m^{-2} s^{-1}). (d) False-coloured image of F_v/F_m at 22.75 hpi of Col-0 plants with DC3000 and DC3000hrpA under 650 µmol m^{-2} s^{-1}. Unlabelled leaves are not infiltrated. Orange represents expected F_v/F_m, whereas yellow/green/blue represents suppressed F_v/F_m. (e) Graph quantifying changes in F_v/F_m over 26.5 hpi of DC3000 on Col-0 under moderate light (650 µmol m^{-2} s^{-1}). Blue represents Col-0 leaves pretreated with H$_2$O; grey—Col-0 leaves pretreated with flg22 (1 µM); yellow line—Col-0 leaves pretreated with elf18 (1 µM). (f) False-coloured image of F_v/F_m for Col-0 plants pretreated with H$_2$O, flg22 (1 µM) and elf18 (1 µM) at 22.75 hpi with DC3000 under 650 µmol m^{-2} s^{-1}. Orange represents expected F_v/F_m, whereas yellow/green/blue represents suppressed F_v/F_m. (g) Graph quantifying changes in F_v/F_m over 26.5 hpi of Col-0 and bak1-5/bkk1-1 leaves with DC3000 under moderate light (650 µmol m^{-2} s^{-1}). Blue represents Col-0 and red bak1-5/bkk1-1 leaves. (h) Image of F_v/F_m 22.75 hpi with DC3000 on Col-0 plant (right) or bak1-5/bkk1-1 plants under 650 µmol m^{-2} s^{-1}. Orange represents expected F_v/F_m, whereas yellow/green/blue represents suppressed F_v/F_m. [Color figure can be viewed at wileyonlinelibrary.com]

fls2 in comparison to Col-0 plants under moderate light (Figure 7). This apparent insensitivity of fls2 plants at moderate light conditions warrants further investigation. Notably, plants preadapted to moderate light were no more or less susceptible than plants exposed to moderate light immediately after the DC3000 challenge (Figure 7 and Supporting Information: Figure 3). Despite visibly showing the presence of anthocyanins, often associated with the accumulation of defensive metabolites (Gould, 2004; Lev-Yadun & Gould, 2008; Schaefer & Rolshausen, 2006), compared to the cognate control plants under 120 µmol m^{-2} s^{-1} (Supporting Information: Figure 3a), plants that had been acclimatized to moderate light treatment for 5 days showed similar enhanced susceptibility (Supporting Information: Figure 3b). Thus, moderate light preadaptation is not required to elicit

enhanced susceptibility, it is only required coincident with pathogen infection to significantly enhance bacterial growth, and this is additional to that achieved by uncoupling classical MTI defences.

3.6 | Pathogen-induced suppression of ABA enhances F_v/F_m reduction

ABA biosynthesis and signalling are hijacked by DC3000 to suppress immunity (de Torres Zabala et al., 2007, 2009). The impact of ABA mutants on virulence is reflected in F_v/F_m signatures (de Torres Zabala et al., 2015). As ABA is made predominantly in the chloroplasts, we investigated whether moderate light-induced
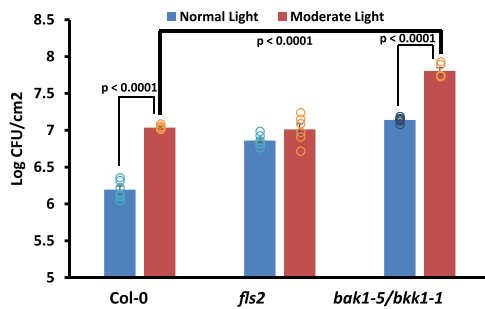
FIGURE 7 Moderate light renders Col-0 and *bak1-5/bkk1-1* plants more susceptible to bacterial infection. Bacterial growth of DC3000 on Col-0, *fls2* and *bak1-5/bkk1-1* plants under normal light (NL; blue; 120 µmol m^{-2} s^{-1}) and moderate light (ML; red; 450 µmol m^{-2} s^{-1}). Error bars, mean ± SE ($n = 6$), Student's *t*-test determined the statistical significance of $p < 0.0001$ for NL Col-0 versus *fls2* and Col-0 versus *bak1-5/bkk1-1* (not shown on graph), ML Col-0 versus *bak1-5/bkk1-1*, Col-0 NL versus ML and *bak1-5/bkk1-1* NL versus ML. There was no significant difference between ML Col-0 versus *fls2* and *fls2* NL versus ML. Representative of three biological replicates. [Color figure can be viewed at wileyonlinelibrary.com]

susceptibility was underpinned by ABA signalling. We monitored the impact of an ABA hypersusceptible signalling mutant (triple mutant) or the ABA-insensitive biosynthetic mutant *aao3* on infection under normal and moderate light, monitoring both F_v/F_m and NPQ, the latter measuring the energy released as heat. The *aao3* mutant exhibited less suppression of F_v/F_m during DC3000 infection compared to Col-0 plants, reflected also in slightly lower levels of NPQ in comparison to Col-0 (Figure 8a,b and Supporting Information: Figure 4a,b). By contrast, the hypersensitive triple PP2C mutant (*abi1/abi2/hab1*) shows a faster decrease in F_v/F_m and a stronger increase in NPQ compared to Col-0 (Figure 8a,b and Supporting Information: Figure 4a,b). As previously reported (Rubio et al., 2009; de Torres Zabala et al., 2007, 2009) under normal light conditions *aao3* plants are more resistant to DC3000, while the triple PP2C mutant is more susceptible (Figure 8c). Notably, while Col-0 and *aao3* plants are more susceptible at a light intensity of 450 µmol m^{-2} s^{-1}, there was no enhanced susceptibility evident in the triple PP2C mutant (Figure 8c), implying either ABA signalling is important for moderate light-enhanced susceptibility or the *abi1/abi2/hab1* plants cannot support further bacterial multiplication. In addition, Col-0 plants grown at 450 µmol m^{-2} s^{-1} show accumulation of ABA after 5 days and also at 9 days postinfection with DC3000 compared to no respective increases in ABA under 120 µmol m^{-2} s^{-1} (Supporting Information: Figure 3c). In contrast, the *aao3* plants do not show an increase in ABA under either light regime (Supporting Information: Figure 3c).

To next assess the interaction of ABA and light on chloroplast function during pathogen infection, 10 µM ABA was coinfiltrated with DC3000 into Col-0 leaves. Under normal light, 10 µM ABA coinfiltration enhances the decrease in F_v/F_m levels as previously reported (de Torres Zabala et al., 2015) (Figure 8d,e). Under moderate light, DC3000 coinfiltration with 10 and 100 µM ABA resulted in a

faster decrease of F_v/F_m levels from 3.5 h onwards (Figure 8f,g). To determine whether 10 and 100 µM ABA affected *P. syringae*, DC3000 was plated on Kings B agar containing 0, 10, 50 and 100 µM ABA. Bacterial growth was moderately restricted ($p < 0.0005$) between 10 and 100 µM ABA treatments (Supporting Information: Figure 4c).

4 | DISCUSSION

We had previously shown that MTI significantly alters the expression of photosynthetic and *NECGs* within the first 2 h of challenge with the T3SS deficient nonpathogenic DC3000*hrpA* (Lewis et al., 2015; de Torres Zabala et al., 2015). Notably, this MTI response results in a strong suppression of *NECGs* yet does not significantly reduce the maximum dark-adapted quantum efficiency (F_v/F_m) of PSII (de Torres Zabala et al., 2015) compared to the mock challenge. In comparison, virulent DC3000 can deliver effectors within 2–3 hpi and strongly suppresses F_v/F_m as well as attenuating MTI-induced cROS (de Torres Zabala et al., 2015). Notably, DC3000 significantly reconfigures the expression of *NECG* within 3–4 h of infection (de Torres Zabala et al., 2015), the timing of which coincides with the delivery of effectors into the plant cell.

Priming of plants to reduce bacterial colonization has been previously demonstrated. Zipfel et al. (2006) showed that *A. thaliana* Col-0 plants primed with flg22 or elf18 have reduced bacterial growth after infection with DC3000 compared to mock primed plants. In addition, Wan et al. (2008) showed that chitin pretreatment also protects *A. thaliana* against DC3000 multiplication. Thus, PRRs signal via a common pathway to induce MTI responses such as callose deposition, ROS and MAP Kinase activation. Activated MTI functions across pathogen classes, for example, the fungal MAMP chitin can prime a plant against bacterial infection (Nühse et al., 2000). Here we investigated the impact of such priming on the chloroplast as photosynthetic genes are significantly altered during disease and early immune signalling (Kachroo et al., 2021; Littlejohn et al., 2021). Our data show that priming with flg22, elf18 or chitin fully attenuates suppression of the maximum dark-adapted quantum efficiency of PSII (F_v/F_m) by DC3000. Experiments with the broad-spectrum ROS and NOS (reactive nitrogen species) stain H$_2$DCF-DA show that this protection extends in part to restricting DC3000 suppression of cROS within primed leaves (Figure 3) (de Torres Zabala et al., 2015). In general, plants that have lost a MAMP; FLS2, EFR, CERK1-2 or DAMP receptor, PepR1-1 × 2-1, can sustain normal F_v/F_m during bacterial infection by priming with an alternative M/DAMP that is, *efr*, *cerk1-2* and *pepR1-1 × 2-1* plants retain normal F_v/F_m with flg22 pretreatment (Figures 1, 2, 5e,f and 9). We did observe, however, that Pep1 and 3 provided reduced attenuation of F_v/F_m suppression in *fls2* plants compared to Col-0 (Supporting Information: Figure 2), and unexpectedly, chitin failed to protect F_v/F_m suppression in *fls2* plants (Figures 2e,f and 9), whereas *efr* plants are protected by chitin treatment (Figure 2c,d and 9). These findings highlight specificity between initial downstream signalling
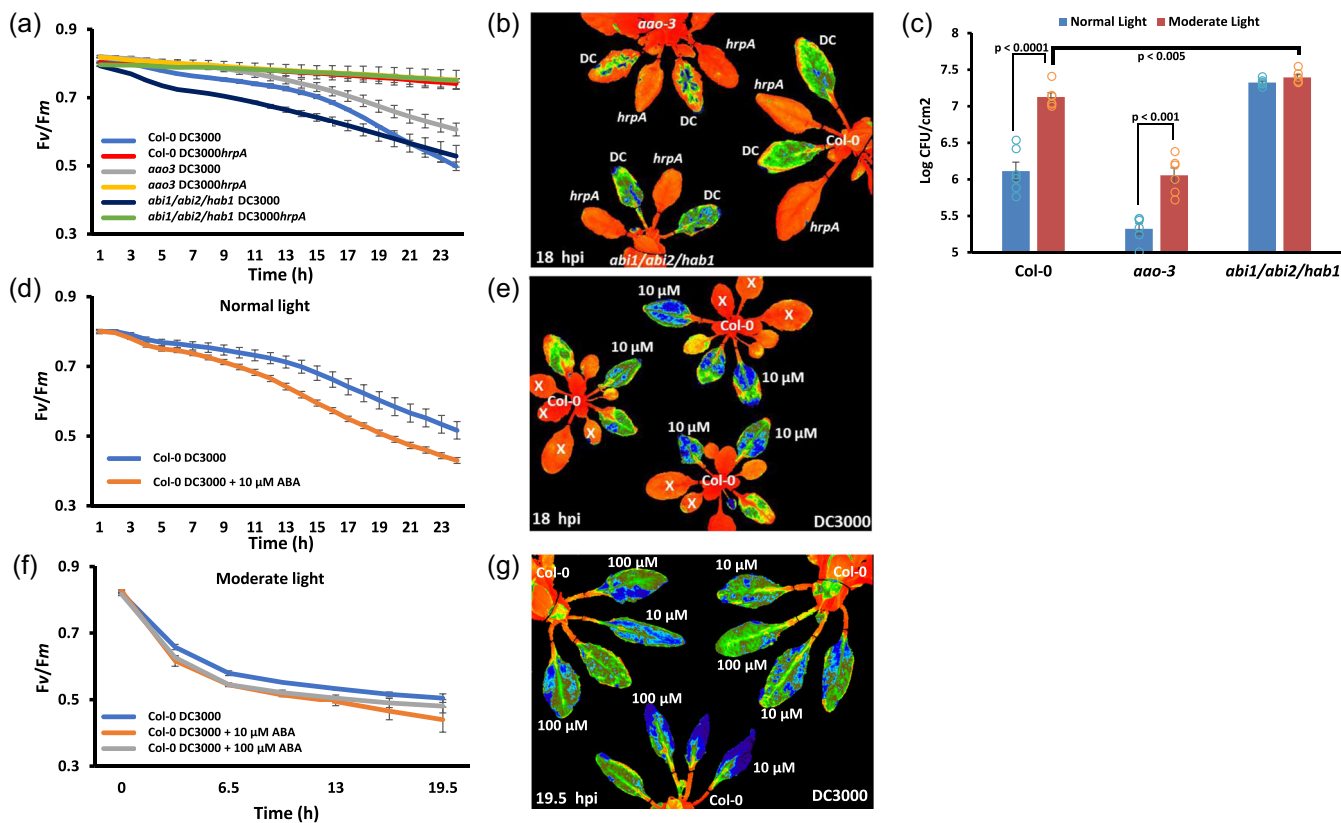
FIGURE 8 Exogeneous abscisic acid (ABA) synergistically or antagonistically alters pathogen-induced ABA suppression of the ratio of variable/maximum fluorescence (F_v/F_m) in a concentration-dependent manner. Bacteria were infiltrated into the leaves on the abaxial side using one infiltration site on either side of the leaf midvein, where undertaken hormones were mixed and coinfiltrated with a bacterial challenge. (a) Graph quantifying changes in F_v/F_m over 24 hours postinfection (hpi) following DC3000 or DC3000hrpA infection of Col-0, aao3 and abi1/abi2/hab1 leaves. Blue represents Col-0 leaves infiltrated with DC3000; red—Col-0 leaves infiltrated with DC3000hrpA; grey—aao3 leaves infiltrated with DC3000; yellow—aao3 leaves infiltrated with DC3000hrpA; dark blue—abi1/abi2/hab1 leaves infiltrated with DC3000 and green corresponds to abi1/abi2/hab1 leaves infiltrated with DC3000hrpA. (b) False-coloured image of F_v/F_m of Col-0, aao3 and abi1/abi2/hab1 plants 18 hpi with DC3000 or DC3000hrpA. Orange represents normal F_v/F_m readout, whereas yellow/green/blue represents suppressed F_v/F_m. (c) Bacterial growth of DC3000 on Col-0, aao3 or abi1/abi2/hab1 plants under normal light (NL; 120 μmol m^{-2} s^{-1}; blue) or moderate light (ML; 450 μmol m^{-2} s^{-1}; orange) conditions. Error bars, mean ± SE ($n = 6$) Student's t-test determined statistical significance of $p < 0.0001$ for Col-0 NL versus ML (shown), statistical significance of $p < 0.001$ for aao3 NL versus ML and statistical significance of $p < 0.005$ for ML Col-0 versus abi1/abi2/hab1. Representative of three replicated experiments. (d) Graph quantifying changes in F_v/F_m 24 hpi with DC3000 on Col-0 leaves in the presence of ABA under normal light (NL; 120 μmol m^{-2} s^{-1}). Blue—Col-0 leaves infiltrated with DC3000 and orange—Col-0 leaves co-infiltrated with DC3000 + 10 μM ABA. (e) False-coloured image of F_v/F_m of Col-0, plants 18 hpi infiltrated with DC3000 and coinfiltrated with DC3000 and 10 μM ABA under NL. Orange represents expected F_v/F_m, whereas yellow/green/blue represents suppressed F_v/F_m. (f) Graph quantifying changes in F_v/F_m up to 24 hpi with DC3000 of Col-0 leaves in the presence of increasing concentrations of ABA under moderate light (ML; 650 μmolm^{-2} s^{-1}). Blue represents Col-0 leaves infiltrated with DC3000; orange—Col-0 leaves coinfiltrated with DC3000+ 10 μM ABA and grey corresponds to Col-0 leaves coinfiltrated with DC3000+ 100 μM ABA. (g) False-coloured image, 19.5 hpi, of F_v/F_m of Col-0 infiltrated with DC3000, coinfiltrated with DC3000 and 10 or 100 μM ABA under 650 μmol m^{-2} s^{-1}. Orange represents expected F_v/F_m, whereas yellow/green/blue represents suppressed F_v/F_m. [Color figure can be viewed at wileyonlinelibrary.com]

through different PRRs. Our data suggest that the activation of immune signals transduced by PepR1/PepR2 and CERK1 are possibly not sufficiently strong to protect against bacterial infection in the absence of FLS2. Notably, in *efr* mutants pretreated with chitin, FLS2 activation could over-ride those chloroplast processes targeted by bacteria during infection, indicating that there may be a requirement for preformed complexes with coreceptors to attenuate chloroplast immune priming.

PRRs represent the first line of induced defence and most require homo or heterodimerisation with a receptor for effective immune

signalling. Chitin induces the dimerization and crosslinking of AtCERK1 which is required for immune signalling (Liu et al., 2012). By comparison, FLS2 and EFR are known to interact with co-receptors BAK1 or BKK1, members of the SERK (SOMATIC EMBRYOGENESIS RECEPTOR KINASEs) protein family. Perception of flg22 or elf18 by their ligand leads to phosphorylation of their intracellular kinase domains and induction of downstream immune signals (Zhang & Zhou, 2010). BAK1 was originally identified as the coreceptor for the BR cell surface receptor BRI1. MTI is impaired in *bak1-5* in response to flg22, elf18 or Pep1, leading to a reduced ROS
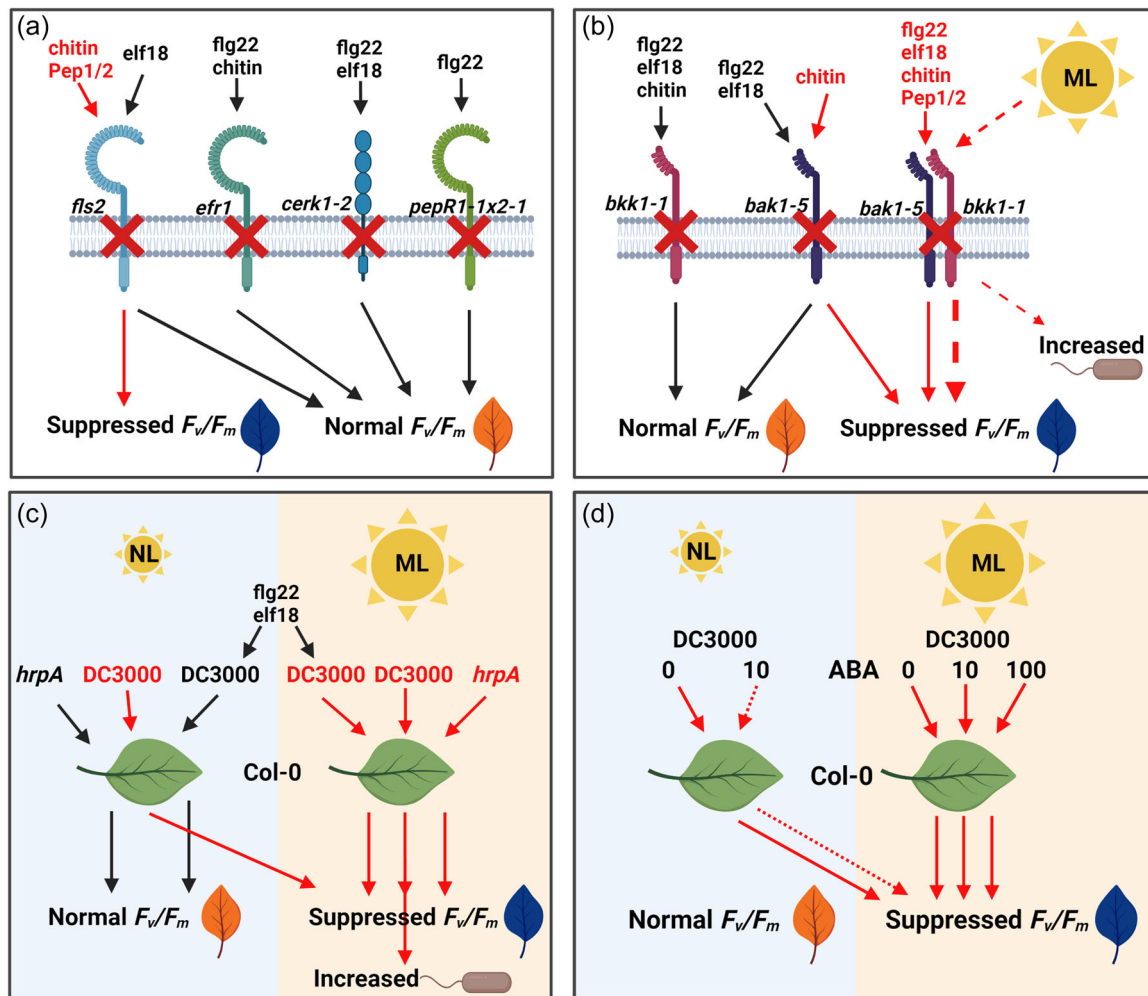
FIGURE 9 Schematic overview of findings from the study. Black arrows show pathways to normal ratio of variable/maximum fluorescence (F_v/F_m), while red arrows show pathways to suppressed F_v/F_m or increased bacterial growth. (a) MAMP pretreatment followed by DC3000 infection on receptor mutant plants. *fls2* leaves pretreated with elf18 maintain normal F_v/F_m, while fls2 leaves pretreated with chitin, Pep1 or 2 show suppressed F_v/F_m. *efr1* leaves pretreated with flg22 or chitin maintain normal F_v/F_m. *cerk1-2* leaves pretreated with flg22 or elf18 maintain normal F_v/F_m. *PepR1-1 × 2-1* leaves with flg22 maintain normal F_v/F_m. (b) MAMP pretreatment followed by DC3000 infection on MTI coreceptor mutant plants. *bak1-5* leaves pretreated with flg22 or elf18 maintain normal F_v/F_m, while *bak1-5* leaves pretreated with chitin show suppressed F_v/F_m. *bkk1-1* leaves pretreated with flg22, elf18 or chitin maintain normal F_v/F_m. *bak1-5/bkk1-1* leaves pretreated with flg22, elf18, chitin, Pep1 or 2 show suppressed F_v/F_m. Under moderate light (ML) conditions (dashed red line), *bak1-5/bkk1-1* leaves show an increased suppression of F_v/F_m (thick, red dashed arrow) and increased bacterial growth compared to normal light (NL) conditions. (c) Chlorophyll fluorescence and bacterial growth are altered under different light conditions. Under normal light (NL; 120 μmol m^{-2} s^{-1}) conditions DC3000hrpA-infected leaves maintain normal F_v/F_m, while DC3000-infected leaves show suppressed F_v/F_m. Pretreatment of Col-0 leaves with flg22 or elf18 under NL results in normal F_v/F_m. Under moderate light (ML; 650 μmol m^{-2} s^{-1}) DC3000hrpA, DC3000 and flg22 or elf18 pretreated DC3000-infected leaves all show suppressed F_v/F_m and DC3000-infected leaves show an increase in bacterial growth. (d) Chlorophyll fluorescence is reduced during moderate light and ABA treatment. Under normal light (NL; 120 μmol m^{-2} s^{-1}) conditions DC3000-infected leaves and leaves coinfiltrated with DC3000+ 10 μM show suppressed F_v/F_m. Under moderate light (ML; 650 μmol m^{-2} s^{-1}) leaves infected with DC3000, leaves coinfiltrated with DC3000+ 10 μM and leaves coinfiltrated with DC3000+ 100 μM all showed suppressed F_v/F_m. Created with BioRender.com. [Color figure can be viewed at wileyonlinelibrary.com]

burst and dampened MAPK activation (Roux et al., 2011). However, this mutant is not impaired in BR signalling (Schwessinger et al., 2011). In contrast, the ROS burst and MAPK responses to flg22, elf18 or Pep1 elicitation in a loss of function *bkk1-1* mutant are similar to wild type (Roux et al., 2011). Priming of either *bkk1-1* or *bak1-5* individual mutants with flg22 and elf18 shows no suppression of F_v/F_m, indicating that these peptides can protect the PSII function

from bacterial infection (Figures 4 and 9). This is comparable to the immune response functions observed for *bkk1-1* and the BR responses observed for *bak1-5* (Roux et al., 2011; Schwessinger et al., 2011). Chitin peptide priming prevented F_v/F_m suppression by DC3000 in *bkk1-1* plants but provided only partial protection in *bak1-5* plants (Supporting Information: Figure 1a–d and Figure 9), consistent with the compromised immune signalling in *bak1-5*.

The double mutant *bkk1-1/bak1-5* has dramatically reduced immune responses to flg22 and elf18 elicitation (Roux et al., 2011). Here we demonstrated that at the level of chloroplast function, priming with flg22, elf18 or chitin offered no protection. Rather, we measure a quantitative hyper-reduction in F_v/F_m in comparison to Col-0 plants (Figures 4 and 9 and Supporting Information: Figure 1d,e). The fact that chitin only provided partial protection to *bak1-5* and no protection to *bkk1-1/bak1-5* plants is of interest since, to date, the LysM containing chitin receptor CERK1 is not known to use BAK1 or BKK1 for signalling (Liu et al., 2012; Yasuda et al., 2017). These data suggest that additional downstream signals linked to BAK1 are required for CERK1 signalling.

Both the chloroplast and light have an impact on plant resistance. Plants were grown under a low Red:Far-Red ratio, which plants use to detect the proximity of neighbours, are more susceptible to pathogen infection by insects, biotrophic bacteria and necrotrophic fungi (Cerrudo et al., 2012; De Wit et al., 2013; Izaguirre et al., 2006; Moreno et al., 2009) due to the alteration of the defence hormones JA and SA. Exposure of plants to different light wavelengths has also been explored in plant defence. Tomato plants that were exposed to green and red light were more resistant to *Pseudomonas cichorii* JBC1 due to the up-regulation of defence-related genes (Nagendran & Lee, 2015). In addition, nightly red light treatment of tomato plants increased resistance to *P. syringae* DC3000 infection linked to the increased accumulation of SA (Yang et al., 2015). Exposure of plants to increasing light intensities causes rapid changes in nuclear gene expression in a photosynthesis-dependent manner and is associated with chloroplast-to-nucleus retrograde signalling (Exposito-Rodriguez et al., 2017; Suzuki et al., 2012; Vogel et al., 2014). A 1 h high light treatment of *Nicotiana benthamiana* reduced F_v/F_m from 0.7 to 0.5 (Exposito-Rodriguez et al., 2017), a much more significant drop than we see with *A. thaliana* over a 3.5 h period (Figure 6c), most likely associated with the higher light intensity of 1000 $\mu mol\,m^{-2}\,s^{-1}$ compared to 650 $\mu mol\,m^{-2}\,s^{-1}$ used in this study. Notably, this drop in F_v/F_m was accompanied by a 50% increase in H_2O_2 (Exposito-Rodriguez et al., 2017). A genetically encoded H_2O_2 reporter localised to the stroma and nucleus revealed that high light treatment (1000 $\mu mol\,m^{-2}\,s^{-1}$) induced H_2O_2 production in these organelles for up to 1 h, and critically, the increase in nuclear H_2O_2 was dependent on electrons from the chloroplast (Exposito-Rodriguez et al., 2017). High light conditions also induced perinuclear clustering of seven to eight chloroplast per nucleus, a similar observation as has been reported for plant–virus interactions (Caplan et al., 2015; Ding et al., 2019). It is predicted that this physical localization facilitates the rapid diffusion of H_2O_2 from chloroplast to nucleus, which elicits an alteration in nuclear gene expression (Exposito-Rodriguez et al., 2017), and it would be interesting to compare the differences in these parameters between DC3000 challenged leaves at 120 and 650 $\mu mol\,m^{-2}\,s^{-1}$.

While excess light is classically associated with enhanced resistance (Kangasjarvi et al., 2012; Karpinski et al., 2013) under moderate light, we unexpectedly found a synergistic effect with effector-mediated suppression of F_v/F_m. Critically, MAMP

pretreatment or ABA coinfiltration fails to attenuate this suppression during DC3000 infection (Figures 6a–f, 7f,g and 9). F_v/F_m levels during a DC3000*hrpA* infection also reduced significantly during the first 6 h of moderate light but recovered to 0.7, compared to 0.75 under normal light (Figure 6a–d). Furthermore, the coreceptor double mutant, *bkk1-1/bak1-5*, also showed increased F_v/F_m suppression compared to wild type following DC3000 challenge, which was accentuated under moderate light (Figure 6g,h). Strikingly, contrary to expectations given the elevated H_2O_2 production, Col-0, *aao3* and *bkk1-1/bak1-5* lines all showed a significant increase in bacterial growth under moderate light but the hypersensitive *abi1/abi2/hab1* mutant and flg22-insensitive mutant *fls2* showed no increase in susceptibility (Figures 7 and 8c). How and why these lines are insensitive to these elevated light conditions warrant further investigation.

Complex plant hormone synthesis and signalling crosstalk play an important role in the outcome of plant disease and defence responses. Both SA and JA are considered key hormones involved in plant immunity; however, it has become apparent in recent years that ABA has a significant role to play in hormone manipulation during pathogen infection (Robert-Seilaniantz et al., 2011). Many organisms produce ABA, from cyanobacteria and fungi to humans, with kingdom-specific synthesis pathways. In plants, ABA is synthesized from carotenoids within the chloroplast, with the final two enzymatic reactions in the cytosol (Finkelstein, 2013; Schwartz et al., 2003). As part of its virulence strategy, *P. syringae* induces de novo ABA biosynthesis in planta and this acts in part by suppressing SA biosynthesis and SA-mediated defences to aid disease progression (Salomon et al., 2014; de Torres Zabala et al., 2007, 2009). Application of exogenous ABA (or coronatine) also induces the expression of the genes encoding three PP2Cs, HAI (HIGHLY ABA-INDUCED) 1, HAI2 and HAI3, all of which interact with and inactivate MPK3 and MPK6, resulting in ABA-mediated MPK3/MPK6 immune suppression (Mine et al., 2017). The PP2C triple mutant, *abi1/abi2/hab1*, is ABA hypersensitive and has enhanced susceptibility to DC3000, whereas the ABA biosynthetic mutant *aao3* shows enhanced disease resistance (de Torres Zabala et al., 2007, 2009). Chlorophyll fluorescence allows dissection of the dynamics of these mutants during DC3000 infection, with the triple mutant exhibiting a stronger suppression of F_v/F_m (and a faster increase in NPQ), while the converse is true for the *aao3* mutant compared to Col-0 (Figure 7a,b and Supporting Information: Figure 3) (de Torres Zabala et al., 2015). Notably, endogenous and exogenous ABA differentially impact apoplastic ROS production, with flg22 challenge of transgenic lines overexpressing ABA resulting in increased apoplastic H_2O_2 production, whereas plants with reduced ABA levels produced less apoplastic H_2O_2 following flg22 treatment (Tan et al., 2019). By contrast, ABA pretreatment resulted in a reduction in flg22-induced apoplastic H_2O_2, indicating that endogenous and exogenous ABA function differently during MAMP-induced apoplastic ROS burst in *A. thaliana* (Tan et al., 2019). During a DC3000*hrpA* infection, cROS is produced at 3–4 hpi, whereas DC3000 infection suppresses cROS, but not when primed with elf18 or flg22 (Figure 3a,b) (de Torres

Zabala et al., [2015]). Unexpectedly, cROS generation appeared ABA dose-dependent, as leaves coinfiltrated with DC3000 and 10 μM ABA elicited a faster decrease of F_v/F_m (similar to the hypersensitive abi1/abi2/hab1 mutants).

Collectively, these data show that F_v/F_m is a reliable, quantitative, real-time indicator of pathogen infection and that abiotic factors affecting chloroplast functions, for example, light and ABA (induced during drought and other abiotic stresses) are generally associated with reduced tolerance to bacterial infection.

ACKNOWLEDGEMENTS

CONFLICT OF INTEREST

The authors declare no conflict of interest.

ORCID

Murray Grant ⓘ http://orcid.org/0000-0003-3357-0264

REFERENCES

Baker, N.R. (2008) Chlorophyll fluorescence: a probe of photosynthesis in vivo. *Annual Review of Plant Biology*, 59(1), 89–113. Available from: https://doi.org/10.1146/annurev.arplant.59.032607.092759

Breeze, E. & Mullineaux, P.M. (2022) The passage of H_2O_2 from chloroplasts to their associated nucleus during retrograde signalling: reflections on the role of the nuclear envelope. *Plants*, 11(4), 552. Available from: https://doi.org/10.3390/PLANTS11040552

Caplan, J.L., Kumar, A.S., Park, E., Padmanabhan, M.S., Hoban, K., Modla, S. et al. (2015) Chloroplast stromules function during innate immunity. *Developmental Cell*, 34(1), 45–57. Available from: https://doi.org/10.1016/j.devcel.2015.05.011

Cerrudo, I., Keller, M.M., Cargnel, M.D., Demkura, P.V., de Wit, D. & Patitucci, M.S. et al. (2012) Low Red/Far-Red ratios reduce *Arabidopsis* resistance to *Botrytis cinerea* and jasmonate responses via a COI1-JAZ10-dependent, salicylic acid-independent mechanism. *Plant Physiology*, 158(4), 2042–2052. Available from: https://doi.org/10.1104/PP.112.193359

Ding, X., Jimenez-Gongora, T., Krenz, B. & Lozano-Duran, R. (2019) Chloroplast clustering around the nucleus is a general response to pathogen perception in *Nicotiana benthamiana*. *Molecular Plant Pathology*, 20(9), 1298–1306. Available from: https://doi.org/10.1111/MPP.12840

Exposito-Rodriguez, M., Laissue, P.P., Yvon-Durocher, G., Smirnoff, N. & Mullineaux, P.M. (2017) Photosynthesis-dependent H_2O_2 transfer from chloroplasts to nuclei provides a high-light signalling mechanism. *Nature Communications*, 8, 1–10. Available from: https://doi.org/10.1038/s41467-017-00074-w

Finkelstein, R. (2013) Abscisic acid synthesis and response. *The Arabidopsis Book*, 11, e0166. Available from: https://doi.org/10.1199/tab.0166

Foyer, C.H. & Hanke, G. (2022) Abiotic stress and adaptation of electron transport: regulation of the production and processing of ROS signals in chloroplasts. *Photosynthesis in Action: Harvesting Light, Generating Electrons, Fixing Carbon* (pp. 85–102). Available from: https://doi.org/10.1016/B978-0-12-823781-6.00010-1

Gould, K.S. (2004) Nature's Swiss army knife: the diverse protective roles of anthocyanins in leaves. *Journal of Biomedicine and Biotechnology*, 2004(5), 314–320. Available from: https://doi.org/10.1155/S1110724304406147

He, K., Gou, X., Yuan, T., Lin, H., Asami, T., Yoshida, S. et al. (2007) BAK1 and BKK1 regulate brassinosteroid-dependent growth and brassinosteroid-independent cell-death pathways. *Current Biology*, 17(13), 1109–1115. Available from: https://doi.org/10.1016/j.cub.2007.05.036

Holt, N.E., Fleming, G.R. & Niyogi, K.K. (2004) Toward an understanding of the mechanism of nonphotochemical quenching in green plants. *Biochemistry*, 43(26), 8281–8289. Available from: https://doi.org/10.1021/bi0494020

Huffaker, A., Pearce, G. & Ryan, C.A. (2006) An endogenous peptide signal in *Arabidopsis* activates components of the innate immune response. *Proceedings of the National Academy of Sciences of the United States of America*, 103(26), 10098–10103. Available from: https://doi.org/10.1073/pnas.0603727103

Izaguirre, M.M., Mazza, C.A., Biondini, M., Baldwin, I.T. & Ballaré, C.L. (2006) Remote sensing of future competitors: impacts on plants defenses. *Proceedings of the National Academy of Sciences of the United States of America*, 103(18), 7170–7174. Available from: https://doi.org/10.1073/PNAS.0509805103

Jin, L., Ham, J.H., Hage, R., Zhao, W., Soto-Hernández, J., Lee, S.Y. et al. (2016) Direct and indirect targeting of PP2A by conserved bacterial Type-III effector proteins. *PLoS Pathogens*, 12(5), e1005609. Available from: https://doi.org/10.1371/journal.ppat.1005609

Jones, J.D.G. & Dangl, J.L. (2006) The plant immune system. *Nature*, 444(7117), 323–329. Available from: https://doi.org/10.1038/nature05286

Jones, J.D.G., Vance, R.E. & Dangl, J.L. (2016) Intracellular innate immune surveillance devices in plants and animals. *Science*, 354(6316), aaf6395. Available from: https://doi.org/10.1126/science.aaf6395

Kachroo, P., Burch-Smith, T.M. & Grant, M. (2021) An emerging role for chloroplasts in disease and defense. *Annual Review of Phytopathology*, 59, 423–445. Available from: https://doi.org/10.1146/ANNUREV-PHYTO-020620-115813

Kangasjarvi, S., Neukermans, J., Li, S., Aro, E.M. & Noctor, G. (2012) Photosynthesis, photorespiration, and light signalling in defence responses. *Journal of Experimental Botany*, 63(4), 1619–1636. Available at https://doi.org/10.1093/jxb/err402

Karpinski, S., Szechyńska-Hebda, M., Wituszyńska, W. & Burdiak, P. (2013) Light acclimation, retrograde signalling, cell death and immune defences in plants. *Plant, Cell & Environment*, 36(4), 736–744. Available from: https://doi.org/10.1111/PCE.12018

King, E.D., Ward, M.K. & Raney, D.E. (1954) Two simple media for the demonstration of pyo-cyanin and fluorescin. *Journal of Laboratory and Clinical Medicine*, 44, 301–307.

Lev-Yadun, S. & Gould, K.S. (2008) Role of anthocyanins in plant defence. In: C. Winefield, K. Davies, & K. Gould (Eds.), *Anthocyanins* (pp. 22–28). Springer. Available from: https://doi.org/10.1007/978-0-387-77335-3_2

Lewis, L.A., Polanski, K., de Torres-Zabala, M., Jayaraman, S., Bowden, L., Moore, J. et al. (2015) Transcriptional dynamics driving MAMP-triggered immunity and pathogen effector-mediated immunosuppression in *Arabidopsis* leaves following infection with *Pseudomonas syringae* pv tomato DC3000. *The Plant Cell*, 27(11), 3038–3064. Available from: https://doi.org/10.1105/tpc.15.00471

Littlejohn, G.R., Breen, S., Smirnoff, N. & Grant, M. (2021) Chloroplast immunity illuminated. *New Phytologist*, 229(6), 3088–3107. Available from: https://doi.org/10.1111/nph.17076

Littlejohn, G.R., Gouveia, J.D., Edner, C., Smirnoff, N. & Love, J. (2010) Perfluorodecalin enhances in vivo confocal microscopy resolution of

Arabidopsis thaliana mesophyll. *The New Phytologist*, 186(4), 1018–1025. Available from: https://doi.org/10.1111/j.1469-8137.2010.03244.x

Liu, T., Liu, Z., Song, C., Hu, Y., Han, Z., She, J. et al. (2012) Chitin-induced dimerization activates a plant immune receptor. *Science*, 336(6085), 1160–1164. Available from: https://doi.org/10.1126/science.1218867

Lu, Y. & Tsuda, K. (2021) Intimate association of PRR- and NLR-mediated signaling in plant immunity. *Molecular Plant–Microbe Interactions*, 34(1), 3–14. Available from: https://doi.org/10.1094/MPMI-08-20-0239-IA

Maruta, N., Burdett, H., Lim, Y. J., Hu, X., Desa, S. & Manil, M.K. et al. (2022) Structural basis of NLR activation and innate immune signalling in plants. *Immunogenetics*, 74(1), 5–26. Available from: https://doi.org/10.1007/S00251-021-01242-5

Miller, G., Schlauch, K., Tam, R., Cortes, D., Torres, M.A., Shulaev, V. et al. (2009) The plant NADPH oxidase RBOHD mediates rapid systemic signaling in response to diverse stimuli. *Science Signaling*, 2(84), ra45. Available from: https://doi.org/10.1126/scisignal.2000448

Mine, A., Berens, M.L., Nobori, T. & Tsuda, K. (2017) Pathogen exploitation of an abscisic acid- and jasmonate-inducible MAPK phosphatase and its interception by *Arabidopsis* immunity. *Proceedings of the National Academy of Sciences of the United States of America*, 114(28), 7456–7461. Available from: https://doi.org/10.1073/PNAS.1702613114

Moreno, J.E., Tao, Y., Chory, J. & Ballaré, C.L. (2009) Ecological modulation of plant defense via phytochrome control of jasmonate sensitivity. *Proceedings of the National Academy of Sciences of the United States of America*, 106(12), 4935–4940. Available from: https://doi.org/10.1073/pnas.0900701106

Nagendran, R. & Lee, Y.H. (2015) Green and red light reduces the disease severity by *Pseudomonas cichorii* JBC1 in tomato plants via upregulation of defense-related gene expression. *Phytopathology*, 105(4), 412–418. Available from: https://doi.org/10.1094/PHYTO-04-14-0108-R

Ngou, B., Ahn, H.K., Ding, P. & Jones, J. (2021) Mutual potentiation of plant immunity by cell-surface and intracellular receptors. *Nature*, 592(7852), 110–115. Available from: https://doi.org/10.1038/s41586-021-03315-7

Nguyen, Q.M., Iswanto, A.B.B., Son, G.H. & Kim, S.H. (2021) Recent advances in effector-triggered immunity in plants: new pieces in the puzzle create a different paradigm. *International Journal of Molecular Sciences*, 22(9), 4709. Available from: https://doi.org/10.3390/IJMS22094709

Noman, A., Aqeel, M. & Lou, Y. (2019) PRRs and NB-LRRs: from signal perception to activation of plant innate immunity. *International Journal of Molecular Sciences*, 20(8), 1882. Available from: from: https://doi.org/10.3390/IJMS20081882

Nühse, T.S., Peck, S.C., Hirt, H. & Boller, T. (2000) Microbial elicitors induce activation and dual phosphorylation of the *Arabidopsis thaliana* MAPK 6*. *Journal of Biological Chemistry*, 275(11), 7521–7526. Available from: https://doi.org/10.1074/jbc.275.11.7521

Robert-Seilaniantz, A., Grant, M. & Jones, J.D.G. (2011) Hormone crosstalk in plant disease and defense: more than just JASMONATE-SALICYLATE antagonism. *Annual Review of Phytopathology*, 49, 317–343. Available from: https://doi.org/10.1146/ANNUREV-PHYTO-073009-114447

Roux, M., Schwessinger, B., Albrecht, C., Chinchilla, D., Jones, A., Holton, N. et al. (2011) The *Arabidopsis* leucine-rich repeat receptor-like kinases BAK1/SERK3 and BKK1/SERK4 are required for innate immunity to hemibiotrophic and biotrophic pathogens. *The Plant Cell*, 23(6), 2440–2455. Available from: https://doi.org/10.1105/tpc.111.084301

Rubio, S., Rodrigues, A., Saez, A., Dizon, M.B., Galle, A. & Kim, T.-H. et al. (2009) Triple loss of function of protein phosphatases type 2C leads to partial constitutive response to endogenous abscisic acid. *Plant Physiology*, 150(3), 1345–1355. Available from: https://doi.org/10.1104/PP.109.137174

Salomon, M.V., Bottini, R., de Souza Filho, G.A., Cohen, A.C., Moreno, D. & Gil, M. et al. (2014) Bacteria isolated from roots and rhizosphere of *Vitis vinifera* retard water losses, induce abscisic acid accumulation and synthesis of defense-related terpenes in in vitro cultured grapevine. *Physiologia Plantarum*, 151(4), 359–374. Available from: https://doi.org/10.1111/PPL.12117

Schaefer, H.M. & Rolshausen, G. (2006) Plants on red alert: do insects pay attention. *BioEssays*, 28, 65–71. Available from: https://doi.org/10.1002/bies.20340

Schwartz, S.H., Qin, X. & Zeevaart, J.A.D. (2003) Elucidation of the indirect pathway of abscisic acid biosynthesis by mutants, genes, and enzymes. *Plant Physiology*, 131(4), 1591–1601. Available from: https://doi.org/10.1104/PP.102.017921

Schwessinger, B., Roux, M., Kadota, Y., Ntoukakis, V., Sklenar, J., Jones, A. et al. (2011) Phosphorylation-dependent differential regulation of plant growth, cell death, and innate immunity by the regulatory receptor-like kinase BAK1. *PLoS Genetics*, 7(4), e1002046. Available from: https://doi.org/10.1371/journal.pgen.1002046

Shine, M.B., Xiao, X., Kachroo, P. & Kachroo, A. (2019) Signaling mechanisms underlying systemic acquired resistance to microbial pathogens. *Plant Science*, 279, 81–86. Available from: https://doi.org/10.1016/j.plantsci.2018.01.001

de Souza, A., Wang, J.-Z. & Dehesh, K. (2017) Retrograde signals: integrators of interorganellar communication and orchestrators of plant development. *Annual review of plant biology*, 68(1), 85–108. Available from: https://doi.org/10.1146/annurev-arplant-042916-041007

Suzuki, N., Koussevitzky, S., Mittler, R. & Miller, G. (2012) ROS and redox signalling in the response of plants to abiotic stress. *Plant, Cell & Environment*, 35(2), 259–270. Available from: https://doi.org/10.1111/j.1365-3040.2011.02336.x

Szechyńska-Hebda, M. & Karpiński, S. (2013) Light intensity-dependent retrograde signalling in higher plants. *Journal of Plant Physiology*, 170(17), 1501–1516. Available from: https://doi.org/10.1016/J.JPLPH.2013.06.005

Tan, L., Liu, Q., Song, Y., Zhou, G., Luan, L. & Weng, Q. et al. (2019) Differential function of endogenous and exogenous abscisic acid during bacterial pattern-induced production of reactive oxygen species in *Arabidopsis*. *International Journal of Molecular Sciences*, 20(10), 2544. Available from: https://doi.org/10.3390/ijms20102544

de Torres Zabala, M., Bennett, M.H., Truman, W.H. & Grant, M.R. (2009) Antagonism between salicylic and abscisic acid reflects early host–pathogen conflict and moulds plant defence responses. *The Plant Journal*, 59(3), 375–386. Available from: https://doi.org/10.1111/J.1365-313X.2009.03875.X

de Torres Zabala, M., Littlejohn, G., Jayaraman, S., Studholme, D., Bailey, T. & Lawson, T. et al. (2015) Chloroplasts play a central role in plant defence and are targeted by pathogen effectors. *Nature Plants*, 1(6), 15074. Available from: https://doi.org/10.1038/NPLANTS.2015.74

de Torres-Zabala, M., Truman, W., Bennett, M.H., Lafforgue, G., Mansfield, J.W. & Egea, P.R. et al. (2007) *Pseudomonas syringae* pv. tomato hijacks the *Arabidopsis* abscisic acid signalling pathway to cause disease. *The EMBO Journal*, 26(5), 1434–1443. Available from: https://doi.org/10.1038/SJ.EMBOJ.7601575

Truman, W., de Torres Zabala, M. & Grant, M. (2006) Type III effectors orchestrate a complex interplay between transcriptional networks to modify basal defence responses during pathogenesis and resistance.

The Plant Journal, 46(1), 14–33. Available from: https://doi.org/10.1111/j.1365-313X.2006.02672.x

Vogel, M.O., Moore, M., König, K., Pecher, P., Alsharafa, K., Lee, J. et al. (2014) Fast retrograde signaling in response to high light involves metabolite export, MITOGEN-ACTIVATED PROTEIN KINASE6, and AP2/ERF transcription factors in *Arabidopsis*. *The Plant Cell*, 26(3), 1151–1165. Available from: https://doi.org/10.1105/tpc.113.121061

Wan, J., Zhang, X.C., Neece, D., Ramonell, K.M., Clough, S., Kim, S. et al. (2008) A LysM receptor-like kinase plays a critical role in chitin signaling and fungal resistance in *Arabidopsis*. *The Plant Cell*, 20(2), 471–481. Available from: https://doi.org/10.1105/tpc.107.056754

De Wit, M., Spoel, S.H., Sanchez-Perez, G.F., Gommers, C.M.M., Pieterse, C.M.J. & Voesenek, L.A.C.J. et al. (2013) Perception of low red:far-red ratio compromises both salicylic acid- and jasmonic acid-dependent pathogen defences in *Arabidopsis*. *The Plant Journal*, 75(1), 90–103. Available from: https://doi.org/10.1111/TPJ.12203

Xiang, T., Zong, N., Zou, Y., Wu, Y., Zhang, J., Xing, W. et al. (2008) *Pseudomonas syringae* effector AvrPto blocks innate immunity by targeting receptor kinases. *Current Biology*, 18(1), 74–80. Available from: https://doi.org/10.1016/j.cub.2007.12.020

Yamaguchi, Y., Huffaker, A., Bryan, A.C., Tax, F.E. & Ryan, C.A. (2010) PEPR2 is a second receptor for the Pep1 and Pep2 peptides and contributes to defense responses in *Arabidopsis*. *The Plant Cell*, 22(2), 508–522. Available from: https://doi.org/10.1105/tpc.109.068874

Yamaguchi, Y., Pearce, G. & Ryan, C.A. (2006) The cell surface leucine-rich repeat receptor for AtPep1, an endogenous peptide elicitor in *Arabidopsis*, is functional in transgenic tobacco cells. *Proceedings of the National Academy of Sciences of the United States of America*, 103(26), 10104–10109. Available from: https://doi.org/10.1073/pnas.0603729103

Yang, Y.X., Wang, M.M., Yin, Y.L., Onac, E., Zhou, G.F., Peng, S. et al. (2015) RNA-seq analysis reveals the role of red light in resistance against *Pseudomonas syringae* pv. tomato DC3000 in tomato plants. *BMC Genomics*, 16(1), 1–16. Available from: https://doi.org/10.1186/s12864-015-1228-7

Yasuda, S., Okada, K. & Saijo, Y. (2017) A look at plant immunity through the window of the multitasking coreceptor BAK1. *Current Opinion in Plant Biology*, 38, 10–18. Available from: https://doi.org/10.1016/j.pbi.2017.04.007

Yu, X., Feng, B., He, P. & Shan, L. (2017) From chaos to harmony: responses and signaling upon microbial pattern recognition. *Annual Review of Phytopathology*, 55(1), 109–137. Available from: https://doi.org/10.1146/annurev-phyto-080516-035649

Yuan, M., Jiang, Z., Bi, G., Nomura, K., Liu, M., Wang, Y. et al. (2021) Pattern-recognition receptors are required for NLR-mediated plant immunity. *Nature*, 592(7852), 105–109. Available from: https://doi.org/10.1038/s41586-021-03316-6

Zhang, J. & Zhou, J.M. (2010) Plant immunity triggered by microbial molecular signatures. *Molecular Plant*, 3(5), 783–793. Available from: https://doi.org/10.1093/MP/SSQ035

Zhong, Y. & Cheng, Z.-M. (2016) A unique RPW8-encoding class of genes that originated in early land plants and evolved through domain fission, fusion, and duplication. *Scientific Reports*, 6(1), 32923. Available from: https://doi.org/10.1038/srep32923

Zipfel, C., Kunze, G., Chinchilla, D., Caniard, A., Jones, J.D.G. & Boller, T. et al. (2006) Perception of the bacterial PAMP EF-Tu by the receptor EFR restricts *Agrobacterium*-mediated transformation. *Cell*, 125(4), 749–760. Available from: https://doi.org/10.1016/j.cell.2006.03.037

SUPPORTING INFORMATION

Additional supporting information can be found online in the Supporting Information section at the end of this article.